

Article

Gridded Satellite Sounding Retrievals in Operational Weather Forecasting: Product Description and Emerging Applications

Emily Berndt ^{1,*} , Nadia Smith ² , Jason Burks ³, Kris White ⁴, Rebekah Esmaili ² , Arunas Kuciauskas ⁵, Erika Duran ⁶ , Roger Allen ⁷, Frank LaFontaine ⁷ and Jeff Szkodzinski ²

¹ NASA Marshall Space Flight Center/Short-Term Prediction Research and Transition Center, Huntsville, AL 35805, USA

² Science and Technology Corporation/National Oceanic and Atmospheric Administration Joint Polar Satellite System Proving Ground and Risk Reduction Program, Columbia, MD 21046, USA; nadias@stcnet.com (N.S.); rebekah@stcnet.com (R.E.); jeff.szkodzinski@stcnet.com (J.S.)

³ National Weather Service/Cooperative Institute for Research of the Atmosphere/Meteorological Development Lab, Silver Spring, MD 20910, USA; jason.burks@noaa.gov

⁴ National Weather Service/Short-Term Prediction Research and Transition Center, Huntsville, AL 35805, USA; kris.white@noaa.gov

⁵ United States Naval Research Laboratory, Marine Meteorology Division, Monterey, CA 93943, USA; arunas.kuciauskas@nrlmry.navy.mil

⁶ Atmospheric Science Department, Earth System Science Center/Short-Term Prediction Research and Transition Center, University of Alabama in Huntsville, Huntsville, AL 35805, USA; erika.l.duran@nasa.gov

⁷ Jacobs Space Exploration Group/Engineering Services and Science Capability Augmentation/Short-Term Prediction Research and Transition Center, Huntsville, AL 35805, USA; roger.e.allen@nasa.gov (R.A.); frank.j.lafontaine@nasa.gov (F.L.)

* Correspondence: emily.b.berndt@nasa.gov

Received: 27 August 2020; Accepted: 9 October 2020; Published: 12 October 2020



Abstract: The National Aeronautics and Space Administration (NASA) Short-term Prediction Research and Transition Center (SPoRT) has been part of a collaborative effort within the National Oceanic and Atmospheric Administration (NOAA) Joint Polar Satellite System (JPSS) Proving Ground and Risk Reduction (PGRR) Program to develop gridded satellite sounding retrievals for the operational weather forecasting community. The NOAA Unique Combined Atmospheric Processing System (NUCAPS) retrieves vertical profiles of temperature, water vapor, trace gases, and cloud properties derived from infrared and microwave sounder measurements. A new, optimized method for deriving NUCAPS level 2 horizontally and vertically gridded products is described here. This work represents the development of approaches to better synthesize remote sensing observations that ultimately increase the availability and usability of NUCAPS observations. This approach, known as “Gridded NUCAPS”, was developed to more effectively visualize NUCAPS observations to aid in the quick identification of thermodynamic spatial gradients. Gridded NUCAPS development was based on operations-to-research feedback and is now part of the operational National Weather Service display system. In this paper, we discuss how Gridded NUCAPS was designed, how relevant atmospheric fields are derived, its operational application in pre-convective weather forecasting, and several emerging applications that expand the utility of NUCAPS for monitoring phenomena such as fire weather, the Saharan Air Layer, and stratospheric air intrusions.

Keywords: NUCAPS; satellite soundings; weather forecasting; operational applications; retrievals; infrared; CrIS; severe weather; fire weather; tropical weather; stratospheric intrusions

1. Introduction

The National Oceanic and Atmospheric Administration (NOAA) Joint Polar Satellite System (JPSS) Proving Ground and Risk Reduction (PGRR) Program has fostered the development and application of satellite sounding retrievals for the benefit of end users through a “Sounding Initiative” and competitively funded projects. The National Aeronautics and Space Administration (NASA) Short-term Prediction Research and Transition Center (SPoRT; [1]) has been part of this effort since 2014, contributing expertise associated with their research-to-operations/operations-to-research paradigm. As a result of multi-organizational/multi-agency collaborations within the JPSS PGRR Sounding Initiative, hyperspectral infrared satellite sounding retrievals are contributing to operational weather forecasting in novel ways that were not anticipated two decades ago when the first hyperspectral infrared sounder was launched on Aqua in 2002. The implementation of the NOAA Unique Combined Atmospheric Processing System (NUCAPS; [2–4]) soundings in the United States NOAA National Weather Service (NWS) operational environment inspired much of the work within the JPSS PGRR Sounding Initiative, including the product design and applications that we discuss in this paper. The structure of the level 2 environmental data records, as arrays of vertical soundings, has limited the availability and accessibility of NUCAPS-derived products to assess these observations in plan-view for spatial context and has limited their widespread application for short-term weather forecasting. While a few previous studies have developed and demonstrated the feasibility of level 2, plan-view hyperspectral infrared sounder products [5,6] for convective forecasting, these capabilities have not been widely adopted into operational NUCAPS algorithm processing. Although level 3 gridded products are routinely produced and available as standard NUCAPS products, there has been a gap in the development of gridded, level 2 products or standardized approaches to support short-term forecasting/analysis. In addition, the derivation of more specialized fields beyond basic temperature, moisture, and trace gases has traditionally not been produced due to the lack of standard approaches to easily process and derive level 2 products. A new method and concept for the processing and representation of NUCAPS level 2-derived products is presented here. This work represents the development of approaches to better synthesize remote sensing observations that ultimately increase the availability and usability of NUCAPS observations to benefit scientific analysis and applications. The optimization of basic gridding and interpolation methodologies as appropriately applied to NUCAPS data retains their observational characteristics and enables state-of-the-art product development to further support their application in weather analysis and forecasting, allowing the capability to add or develop new derived products easily. The derived products presented herein, represent the novel development of fields not traditionally derived from hyperspectral infrared sounder observations and new concepts/methods to support applications related to short-term weather forecasting and analysis.

The NUCAPS retrieval system is based on version 5.9 of the NASA Atmospheric Infrared Sounder (AIRS) science team method [7] and runs operationally at NOAA with global coverage in near real-time (~180 min latency) and via direct broadcast sites with regional coverage in real-time (<60 min latency). By “operational”, we mean that the system runs continually on every measurement made from space. While NUCAPS has the capability to retrieve soundings from AIRS measurements, it runs operationally at NOAA on measurements made by the Cross-track Infrared Sounder (CrIS), in orbit since 2011 on two different platforms, as well as the Infrared Atmospheric Sounding Interferometer (IASI), in orbit since 2006 on a series of European Meteorological Operational (MetOp) satellite platforms. On any given day at a target scene, there are thus multiple NUCAPS soundings available throughout the diurnal cycle to support any number of applications. Here, we introduce the novel NUCAPS product, known as “Gridded NUCAPS”, and the applications it supports. We distinguish between operational applications with a known user-base in weather forecasting and emerging applications with demonstrated relevance to weather forecasting.

NUCAPS sounding products are operationally available to the NOAA weather forecasting community through the Advanced Weather Interactive Processing System (AWIPS) that ingests and displays data products from a wide array of sources to support weather analysis and forecasting.

In 2014, NUCAPS soundings were officially delivered to the NWS AWIPS system operationally, and for the first time forecasters could visualize hyperspectral infrared sounding observations as “Skew-T” diagrams, or thermodynamic plots of temperature and dewpoint profiles. This is also how forecasters view radiosondes, so comparisons between these two sources are easy and intuitive. With thousands of satellite soundings supplementing the sparse radiosonde network, forecasters suddenly had ready access to wide swaths of satellite soundings that helped them characterize the pre-convective environment, when radiosondes are typically sparse or absent [6,8–12]. To date, NUCAPS remains the only NOAA operational sounding product from hyperspectral infrared measurements and the only product of its kind in AWIPS. With active partnerships in the JPSS PGRR Sounding Initiative and this new data source available to NWS Weather Forecast Offices (WFOs) within the United States (including Alaska, Hawaii, and Puerto Rico), forecasters started applying NUCAPS soundings to different forecasting scenarios, such as the cold air aloft aviation hazard described by Weaver et al. [13]. It was this novel application in aviation weather forecasting that inspired the design of Gridded NUCAPS, which allowed forecasters to visualize incoming swaths of NUCAPS soundings as horizontal or vertical cross-sections, instead of individual soundings one Skew-T diagram at a time. With Gridded NUCAPS, Alaskan forecasters could readily determine the spatial and vertical extent of cold-air aloft features and thus speed up their issuing of warnings to the aviation community. The methodology to ingest and display satellite soundings as a series of values at different pressure levels, instead of vertical profiles, was first developed by [5] and later refined by this team through an iterative process involving end user assessment and feedback [11,13–15] with the current method described below. As a result of operations-to-research feedback and collaborative efforts within the JPSS PGRR Sounding Initiative, AWIPS now has the operational ability to display NUCAPS soundings not only as Skew-T diagrams, but also as plan-views and cross-sections of the three-dimensional atmosphere through the Gridded NUCAPS capability.

Gridded NUCAPS has operational applications in severe weather forecasting because with overpasses from CrIS at 01:30 pm local time, it characterizes the summertime, peak afternoon pre-convective environment with observations between typical radiosonde launches that forecasters can use to evaluate forecast models ahead of afternoon thunderstorms. With Gridded NUCAPS, weather forecasters can visualize horizontal swaths of the retrieved sounding observations at different heights and quickly identify areas of convective instability. Gridded NUCAPS has been evaluated within AWIPS by operational forecasters at the Hazardous Weather Testbed (HWT) annually since 2016 to determine its relevance and applicability and refine its quality [8–11,15–17]. The HWT is one of a number of NOAA test beds [18] designed to facilitate a link between researchers and operational forecasters. Esmaili et al. [11] discussed how our partnership with the NWS through the JPSS PGRR program ensures an effective flow of information between the research and operational communities. There is the “research-to-operations” flow that helps to make science operationally available to decision-makers and the “operations-to-research” flow that inspires operationally relevant research and products tailored to operational applications. The Gridded NUCAPS capability, with its emerging applications that we discuss in this paper, is a testimony to the value of this partnership and flow of information.

The main aim of this work is to highlight the Gridded NUCAPS product design and discuss several emerging applications within the NOAA operational environment and beyond. These new applications are an opportunity for research to have value in operations and, in turn, for operations to inform research and product improvement. Section 2 describes the datasets and methodology we implemented to project the NUCAPS soundings from their instrument grid to a standard latitude/longitude grid (0.5° resolution at a fixed set of vertical levels. Section 3 highlights one operational application—namely, surveilling the pre-convective environment—and three emerging applications, including fire weather analysis, monitoring the Saharan Air Layer (SAL), and identifying stratospheric air influence and tropopause folding. The latter was first conceptualized and demonstrated by [19–21] for the AIRS version 6 suite of

products. Section 4 is a discussion of the significance of this work, while the manuscript is concluded in Section 5.

2. Materials and Methods

2.1. Datasets: NUCAPS Satellite Soundings

We focus here on the NUCAPS retrieved profiles of temperature, moisture, and ozone from CrIS and the Advanced Technology Microwave Sounder (ATMS) on the Suomi-National Polar-orbiting Partnership (S-NPP) and NOAA-20 platforms. NUCAPS is based on the AIRS version 5.9 algorithm [7]. S-NPP NUCAPS soundings were made available to the NWS in 2014 through the satellite broadcast network. Today, only NOAA-20 soundings are made available to the NWS, since the S-NPP CrIS side-b electronics anomaly during 2019 impacted the availability of S-NPP NUCAPS for a short period of time, and its feed into AWIPS was shut off as a result. Although much of this work depends on the real-time delivery of NUCAPS soundings to the NWS, the examples in this work utilize both NOAA-20 and S-NPP NUCAPS data obtained from the NOAA Comprehensive Large Array Stewardship System (CLASS), either reprocessed for AWIPS display or processed and displayed with the Gridded NUCAPS stand-alone python code base.

For use in real-time forecasting, the NUCAPS algorithm was designed to achieve high-quality profiles across the globe, generate traceable error estimates, and maintain a high computational efficiency. NUCAPS is an optimal estimation retrieval system [22]. Optimal estimation is a method employed in many other retrieval systems also [23–27] that adds information from the radiance measurements to an estimate of the atmospheric state (known as the a-priori, or first guess), while propagating error estimates from both sources to the final solution. This technique has been widely adopted because the space-based radiance measurements do not contain enough information to fully resolve the vertical atmospheric state at every retrieval footprint, and an a-priori estimate helps stabilize the solution. An optimal estimation temperature retrieval can, thus, be interpreted as an improvement in prior assumptions about atmospheric temperature based on measurements from space. One can use any number of data sources to function as an a-priori, as seen in these systems [23–27]. NUCAPS calculates an a-priori for temperature, moisture, and ozone by applying regression coefficients to the CrIS/ATMS measurements. These coefficients are calculated off-line as the correlation between four global days of CrIS/ATMS measurements and co-located atmospheric state variables from the European Centre for Medium-range Weather Forecasts (ECMWF) reanalysis model. Even though these regression coefficients have a model dependence, one can regard the regression retrievals from radiance measurements to have a minimal dependence on forecast models because most of the information about the instantaneous atmospheric state is derived from the radiances themselves. NUCAPS uses a linear regression approach, as described by [28], though other approaches exist here [29–33]. Operational meteorologists value the fact that NUCAPS soundings are largely model-independent, because this allows them to verify forecast models in real-time.

NUCAPS is a multi-step retrieval system that we will not describe in-depth, but it is worth highlighting how NUCAPS retrieves soundings in cloudy atmospheres, because this has direct relevance to discussions here. NUCAPS uses a technique called “cloud clearing” [7,24,34] to derive a cloud-free radiance estimate from each cluster of 9 CrIS radiances (3×3 fields of view). This technique is a simple, robust means with which to remove the effects of clouds from the measured radiances without prior knowledge of clouds or the requirement for complex radiative transfer calculations through clouds. With cloud clearing, NUCAPS retrievals in partly cloudy scenes can be interpreted as the state of the atmosphere around or past the clouds, not through the clouds. Cloud clearing does reduce the spatial resolution of NUCAPS retrievals, since a sounding is retrieved for every aggregate of 9 CrIS fields of view (~50 km at nadir and ~150 km at the edge of the scan), but it significantly increases the retrieval yield to a ~75% success rate from a global set of measurements and allows sounding observations in complex, partly cloudy scenes to characterize the environment within storms. Another

aspect of NUCAPS is that it retrieves temperature and moisture twice—first from a microwave-only (MW-only) set of ATMS channels [25,35,36], and second from a set of infrared plus microwave (IR + MW) channels [2,4]. Both MW-only and IR + MW retrievals are part of the NUCAPS product, but only the latter is available in AWIPS. The MW-only retrievals contribute to evaluating whether the IR + MW retrievals failed or succeeded.

2.2. Methods: Gridded NUCAPS Product Design

The current Gridded NUCAPS capability was released in the AWIPS baseline distribution in 2019. AWIPS is the primary visualization and decision-support platform for the NWS WFOs. “Baseline” means that the same configuration and software capability is distributed to all WFOs within the United States. This gives each WFO the ability to generate the same Gridded NUCAPS products from the real-time flow of satellite data into AWIPS. The Gridded NUCAPS capability is still under active development to refine the initial AWIPS capability and to create a robust code base for processing gridded sounding products for real-time web-based visualizations for non-AWIPS users and to support applied research and validation studies.

Before the horizontal grids are created, a vertical interpolation is independently applied to each sounding to interpolate the data to standard pressure levels (P_{std}). In Gridded NUCAPS, the 100 native NUCAPS levels are transformed to standard meteorological levels in the AWIPS operational environment for inter-comparison with other data sets, such as models and radiosondes. The set of standard gridded levels we defined are 41 levels from 1100 to 100 hPa every 25 hPa to match the NWP models and enable easier comparison in AWIPS. The observations are interpolated from the Earth’s surface to 100 hPa with linear interpolation. In NUCAPS, trace gases are retrieved on pressure layers and temperature on pressure levels. Trace gas quantities, such as water vapor and ozone, must first be converted from a layer quantity to a level quantity. The conversion takes the midpoint between two layer quantities to calculate the level quantity, where $V_{lev,i}$ in Equation (1) represents the trace gas variable such as water vapor or ozone and i represents the index of the native 100 NUCAPS pressure levels, where $i = 1$ and $i = 100$ are at the top and bottom of the atmosphere, respectively:

$$V_{lev, i} = \begin{cases} \frac{V_i + V_{i-1}}{2} & i > 1 \\ V_1 & i = 1 \end{cases} \quad (1)$$

Note that index i may be less than 100 for soundings where the topography is higher and surface pressure is lower than 1100 hPa. This methodology is described below. Separate functions (Equations (2) and (3)) are used to interpolate temperature to standard levels ($T_{std,j}$) compared to water vapor and ozone ($V_{std,j}$). To preserve the mass, water vapor and ozone are linearized by interpolating the standard logarithm of the column density. Below, j represents the index of the 41 standard pressure levels where $P_{i-1} \leq P_{std,j} \leq P_i$. Like the index i : $j = 1$ and $j = 41$ are at the top and bottom of the atmospheric column, respectively:

$$T_{std, j} = T_{i-1} + (T_{std, j} - T_{i-1}) \times \frac{P_{std, j} - P_{i-1}}{P_i - P_{i-1}}, \quad (2)$$

$$V_{std, j} = \left[\log_{10}(V_{i-1}) + (\log_{10}(V_{std, j}) - \log_{10}(V_{i-1})) \times \frac{\log_{10}(P_{std, j}) - \log_{10}(P_{i-1})}{\log_{10}(P_i) - \log_{10}(P_{i-1})} \right]^{10} \quad (3)$$

Figure 1a is an example of the impact of the vertical interpolation on the sounding. There are only slight differences between the resampled profile (blue) and the original sounding (pink). With the cold air aloft aviation hazard in mind, critical temperatures < -65 °C (gray shading in Figure 1b,c) are still identified in the vertically interpolated sounding, with only a 10 hPa difference between the bottom of the cold air aloft layer when comparing the interpolated and native NUCAPS temperature. Based on forecaster feedback, the slight differences in the 250–200 hPa layer are not significant enough to impact the integrity of the sounding or drastically change decisions related to forecasting applications.

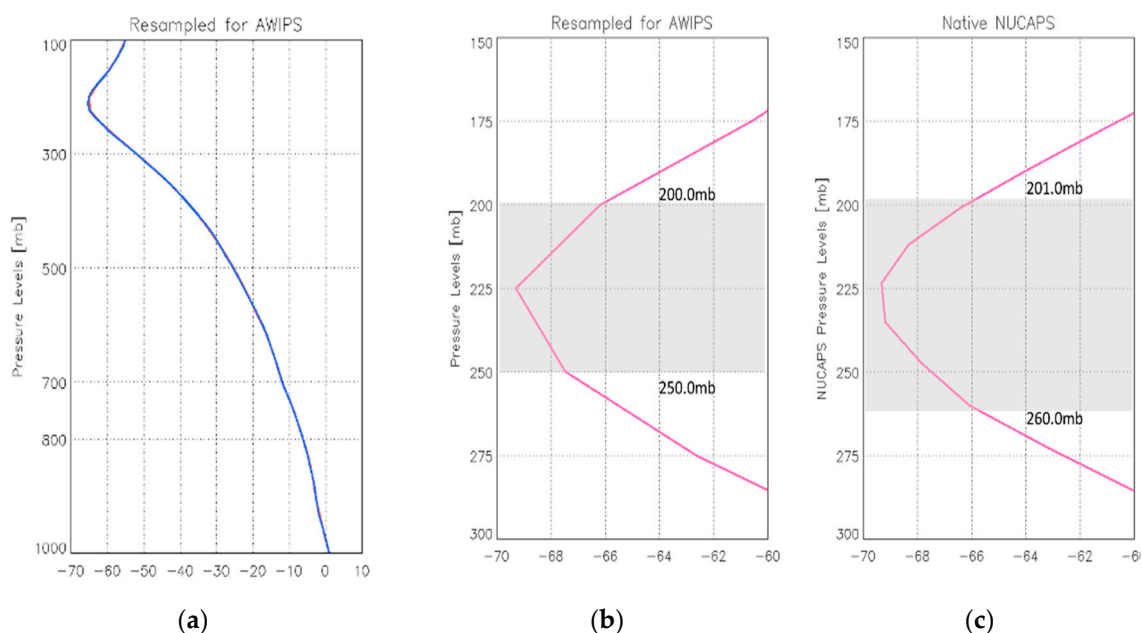


Figure 1. Example of the vertical interpolation compared to the native National Oceanic and Atmospheric Administration (NOAA)'s NOAA Unique Combined Atmospheric Processing System (NUCAPS) resolution. (a) NUCAPS vertical temperature sounding plotted on native 100 levels in blue overlaid on NUCAPS temperature interpolated to 41 standard levels (pink). Comparison of the 300–150 hPa upper-level region between (b) temperature interpolated to 41 vertical levels, and (c) native NUCAPS 100 levels. The gray region represents the region of the sounding $< -65\text{ }^\circ\text{C}$, the criteria for identifying the potential for the cold air aloft aviation hazard.

The horizontal gridding is performed on temperature, relative humidity, and additional derived fields. Each array of aggregated soundings is added to a 0.5° latitude/longitude grid over a global domain using nearest neighbor and minimal interpolation. Regions outside the swath are masked where data are unavailable before the gridding takes place. Horizontal fields are created for temperature and relative humidity on 41 standard levels and at the surface (e.g., 2-m), quality flags, and derived single layer products: total precipitable water (TPW) and layer precipitable water (LPW), total ozone, ozone anomaly, and tropopause level are also gridded. In AWIPS, the data are output as a grid record and made available for display. The derived parameters in AWIPS are leveraged to calculate and display additional fields such as lapse rates, theta-e/theta-e lapse rates, Haines Index, and other stability parameters derived from temperature and moisture. The derived parameters are baseline python functions in AWIPS that perform calculations on model and even satellite data to “derive” fields for display. Given that Gridded NUCAPS is ingested as a grid record, akin to model data, any derived parameter that uses temperature or moisture fields for its derivation can be calculated and displayed. Therefore, a wide array of display fields are available through AWIPS-derived parameters. Some fields derived by AWIPS such as stability indices that rely on levels within the boundary layer still need further evaluation for accuracy and efficacy. The specific variables and levels/layers presented here were chosen based on operations-to-research feedback gathered during annual participation in the HWT spring experiment [11,16,17].

Ideally, prior to vertical interpolation and horizontal gridding, the bottom of each sounding should be found based on comparing the surface pressure to the NUCAPS pressure levels. Correctly adjusting the surface and boundary layer conditions according to local changes in topography and surface pressure benefits the interpretation of satellite soundings and prevents the propagation of systematic uncertainty in derived geophysical variables (i.e., lapse rate, stability indices). Note that NUCAPS sounding files include 100 levels from 1100 hPa (P_{100}) up to top of the atmosphere (0.0016 hPa; P_1),

and 1100 hPa is often below the Earth’s surface and unrepresentative of actual conditions. In the event that the Earth’s surface is higher than P_{100} , the remainder of the pressure grid is filled in with values identical to surface temperature, thus creating an isothermal profile below the surface. The technique outlined in Figure 2 removes any isothermal layer from the NUCAPS sounding and correctly assigns the bottom level. This technique to find the bottom portion of the sounding is implemented in the current AWIPS capability. This technique can be taken one step further to adjust the boundary layer temperature and moisture values in the sounding. The boundary layer multiplier (BLMULT; Equation (4)), can be calculated to either narrow or broaden the boundary layer to within 0.2 to 1.2 hPa. Then, a representative fraction of the temperature or moisture can be added or removed from the bottom of the sounding. Since the NUCAPS level closest to the surface pressure will never be an exact match, BLMULT can account for this discrepancy. BLMULT is calculated by:

$$BLMULT = \frac{P_{surf} - P_{botlev-1}}{P_{botlev} - P_{botlev-1}}, \tag{4}$$

where P is the array of 100 NUCAPS pressure levels, surface pressure (P_{surf}) is obtained from the Global Forecast System as part of the NUCAPS algorithm, and botlev is the bottom-level pressure index found using one of the three conditions in Figure 2. Then, the surface temperature (T_{surf}) is calculated by Equation (5) as follows:

$$T_{surf} = T_{botlev-1} + BLMULT \times [T_{botlev} - T_{botlev-1}]. \tag{5}$$

Note that Equation (5) is modified to calculate the surface relative humidity in the same manner. For the total column fields such as ozone and total precipitable water (V_{tot}), BLMULT is applied to the concentration density at the bottom level (V_{botlev}) and added to the total column:

$$V_{tot} = BLMULT \times V_{botlev} + \sum_{i=1}^{botlev-1} V_i. \tag{6}$$

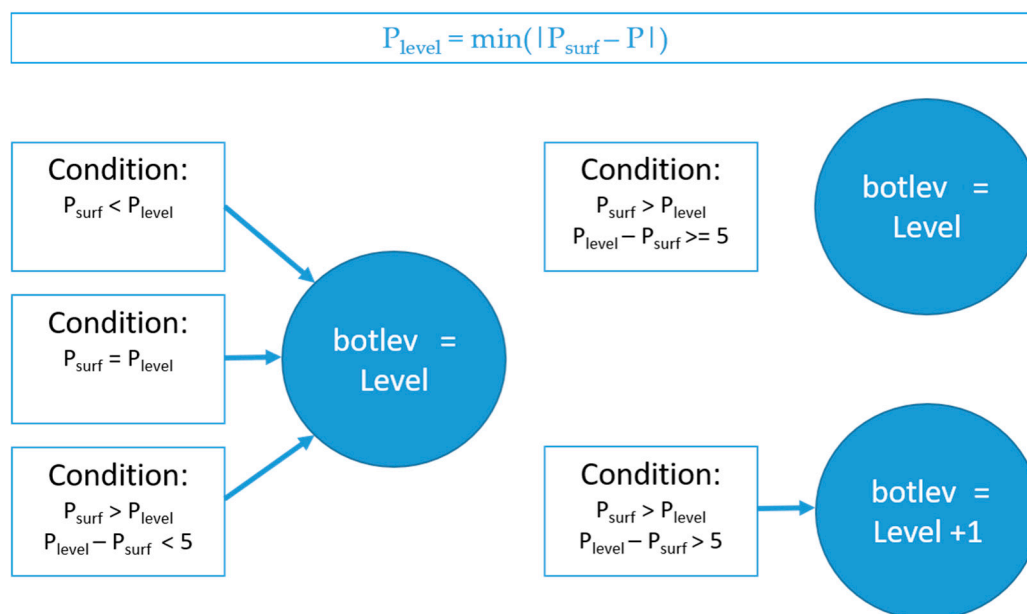


Figure 2. The conditions for finding the index of the bottom level (botlev) in a NUCAPS sounding. Level is the index of the pressure level satisfying $\min(|P_{surf} - P|)$. The index botlev is required for accurately calculating the temperature and trace gas surface values.

Figure 3 is an example application of the surface adjustment and BLMULT to a NUCAPS sounding. With a surface pressure of 1029 hPa, the bottom of the sounding is the 1042 hPa NUCAPS level and BLMULT represents an expansion of the boundary layer by 0.5576 hPa. Note that the isothermal layer starting at 1042 hPa and downward is below the topography. The BLMULT can then be applied to temperature and moisture to adjust the surface value. In this case, the fraction of temperature within the bottom layer is added to the temperature at the specified level (258.318 K at 1013 hPa) for a new surface temperature of 257.774 K. BLMULT was only implemented within TPW and is the lowest LPW field in the Gridded NUCAPS. Active development is underway to fully implement BLMULT in the second iteration of the AWIPS capability and the non-AWIPS visualizations. Currently, the surface or 2-meter temperature and relative humidity are found according to Figure 1 after the data are interpolated to standard levels, but BLMULT is not applied. Note that the isothermal layer is removed before vertical interpolation, but BLMULT was not fully implemented due to the complexity of developing the initial AWIPS plugin. The newer version will use BLMULT to adjust the temperature and moisture of the sounding to find 2 m fields and will apply BLMULT prior to performing any vertical interpolation. Active development is underway to test this with non-AWIPS processing and integrate it in updated AWIPS code.

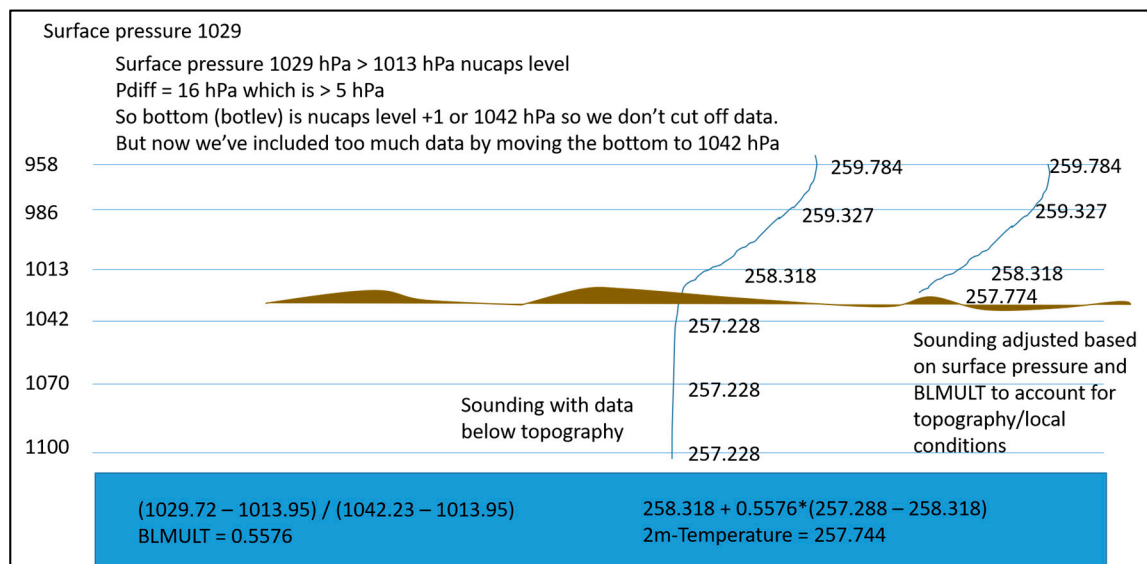


Figure 3. Example of finding the bottom of a sounding, calculation of boundary layer multiplier (BLMULT), and deriving the surface temperature.

2.3. Methods: Gridded NUCAPS-Derived Fields

2.3.1. Lapse Rate

For AWIPS users, the lapse rate is calculated with AWIPS-derived parameters according to the Poisson Equation (Equation (7)). The constant is the result of the division of gravity 9.81 m/s by the gas constant for dry air (287 J/kg·K). $T(P)$ and $T_0(P_0)$ represent temperature (pressure) at the top and bottom of the layer, respectively. The AWIPS menu includes commonly used lower-level and upper-level lapse rates based on feedback from users to promote ease of access. Less commonly used lapse rates are available through the AWIPS product browser. For non-AWIPS tools which do not automatically compute the lapse rate, the lapse rate is pre-calculated for visualization of the 850–500, 700–500, and 400–200 hPa layers, and additional lapse rate calculations can be flexibly added for processing and display.

$$LR = 0.034167 \times \left[\log \frac{T}{T_0} / \log \frac{P}{P_0} \right]. \quad (7)$$

2.3.2. Haines Index

The Haines Index was first described by [37] and further defined by [38], and is calculated with two terms representing stability and moisture. The stability term is assigned a value, 1–3, based on the lapse rate of the identified layer, which is also calculated with Equation (7). The moisture term is assigned a value of 1–3 based on the dew point depression of the defined level. The two values are added to indicate the potential for large fire growth (e.g., 2–3 = very low, 4 = low, 5 = moderate, 6 = high). Werth and Ochoa [38] give suggested layers/levels to derive the Haines Index to account for topography and reduce the influence of the diurnal variability in the surface temperature and associated surface inversions. The AWIPS-derived parameters calculate the Haines Index given the temperature and relative humidity of the NUCAPS grids. These layers/levels can be adjusted in the AWIPS Haines Index-derived parameter. Current development with the Gridded NUCAPS non-AWIPS visualizations includes the derivation of the Haines Index at the suggested layers/levels based on [38].

2.3.3. Precipitable Water

The derivation of precipitable water (TPW and LPW) was included in the initial AWIPS gridding capability. The TPW and LPW represent the water vapor contained in a vertical column of unit cross-sectional area extending between any two specified levels and is expressed in terms of the height the water would stand if completely condensed into the same unit area, as expressed in Equation (8):

$$TPW = \frac{MW_{H_2O}}{N_a} \times \sum_{i=sfc}^{toa} WV_{cd}(i). \quad (8)$$

The water vapor column density is integrated from the top to bottom level following Equation (8), and then multiplied by the molecular mass of water vapor (MW_{H_2O} , 18.0151 g/mol) and divided by Avogadro's number (N_a , $6.02214199 \times 10^{23}$), yielding a value in cm. Precipitable water is calculated over three additional layers (surface–800 hPa, surface–500 hPa, or surface–300 hPa) in the initial version of the AWIPS implementation, with plans to adjust the layer calculations based on user feedback. In AWIPS, forecasters can view TPW or LPW in cm, m, or inches, depending on user preference and editing user configuration files. BLMULT is applied to adjust the bottom of the TPW and LPW fields. Future AWIPS implementation of LPW will include the derivation of the products with the moisture interpolated to standard levels and LPW calculated over familiar layers similar to other satellite-derived PW products (e.g., surface–850, 850–700, 700–500, and 500–300 hPa). The current Gridded NUCAPS web-visualizations and examples below derived from non-AWIPS code include the new LPW layers.

2.3.4. Ozone-Derived Products

As a result of end user feedback within the JPSS PGRR program, several derived products were included in the Gridded NUCAPS development. Previous work by [19] and [20,21] led to the development of ozone-derived products from hyperspectral infrared sounders to support forecasting rapid cyclogenesis and the development of associated high winds and hurricane extratropical transition. The total column ozone is calculated from the ozone mixing ratio and converted to Dobson Units for gridding and display. The ozone anomaly product was developed to identify regions of climatologically high ozone, indicating the presence of stratospheric air and the potential for tropopause folding [21]. The total column ozone is compared to a latitudinal and monthly climatology database developed by [39] to characterize anomalous ozone values. With the knowledge that stratospheric air can be identified where ozone values are at least 25% greater than climatology [40], the percent of normal between 0% and 200% is calculated and displayed with values 125% or greater in shades of blue. The full product derivation and examples are outlined in [21]. The tropopause level product was created as an innovative method of identifying the tropopause in satellite soundings. Since it can be difficult to ascertain the tropopause height by analyzing vertical temperature and moisture profiles due to the smooth nature

of satellite soundings, the use of gridded-plan view ozone products is advantageous. Ozone can be used to identify the height of the tropopause; however, the use of threshold values such as 100 ppb can be misleading due to the seasonal changes in ozone and the tropopause height. Thouret et al. [41] developed a seasonal variation in ozone at the dynamic tropopause, defined as 2 Potential Vorticity Units, using flight observations and model data. The study resulted in the following equation, which is a synthetic definition of the monthly mean climatological ozone value at the tropopause that accounts for the sine seasonal variation with a maximum in May and minimum in November:

$$91 + 28 \times \sin(\pi \times (Month - 2) / 6). \quad (9)$$

With the NUCAPS soundings, the tropopause level is found by matching the level where the ozone value is greater than or equal to the monthly threshold determined by Equation (9) from Thouret et al. [41]. The tropopause level in hPa is then gridded for display.

3. Results

3.1. Surveilling the Pre-Convective Environment

During the 2019 HWT Spring Experiment, NUCAPS soundings were used in the analysis of convection that developed in central Illinois on 5 June [42,43]. A line of storms developed in southern Iowa, and moved southeast into central Illinois by 1600 UTC. Figure 4a shows the Gridded NUCAPS TPW values around 30 mm over the region, while closer analysis of 700–500 hPa LPW indicates a drier layer in southern Illinois. This same dry signature is also evident in the 700 hPa relative humidity. Although not shown, the near-surface LPW and relative humidity fields indicate a relatively moist near-surface environment. The storms developed along a swath of regionally higher LPW and relative humidity, and increased in intensity during the afternoon hours, before decreasing in overall intensity after moving into the environment with drier air in the mid-levels (e.g., around 2200 UTC, approximately 3.5 h after the NOAA-20 overpass). The Storm Prediction Center storm reports indicate that most of the wind damage associated with the line occurred between 2030 and 2220 UTC [44]. This analysis shows the advantage of plan-view analysis to assess the environment, especially with more reliable fields that are above the boundary layer influence. Interrogating individual NUCAPS profiles can provide valuable temperature and moisture measurements, especially above the boundary layer. However, because soundings are volume measurements and not point observations, near the surface the soundings may underestimate important stability indices or features such as inversions when compared with radiosondes. In the June 5 case, the forecaster found NUCAPS vertical sounding Convective Available Potential Energy (CAPE) values were underestimated in the low to mid-levels when compared to the immediate Lincoln, Illinois sounding, which was valid at 1700 UTC [42]. The gridded fields allow the end user to assess the broad environment quickly and above the boundary layer, with a focus on changes in gradients and patterns.

These activities have led to valuable operations-to-research feedback from end users to tailor products to address the needs of the operational environment. One key area of active research is addressing the representation of the boundary layer in satellite soundings. Forecasters need the accurate representation of surface temperature, moisture, and structures such as inversion layers to diagnose the potential for convective development. The representation of temperature and moisture fields is also necessary, since they are used to derive common stability fields such as CAPE, important for diagnosing convective potential and storm-scale updraft strength. Manual and automated techniques have been applied to improve the boundary layer representation of satellite soundings and have been accepted by forecasters as an improvement in the utility of these data in operations [11,45]. There are ongoing efforts by NUCAPS developers to improve the boundary representation within the retrieval algorithm and as a post-processing step within target applications. An in-depth discussion of these efforts is, however, beyond the scope of this paper.

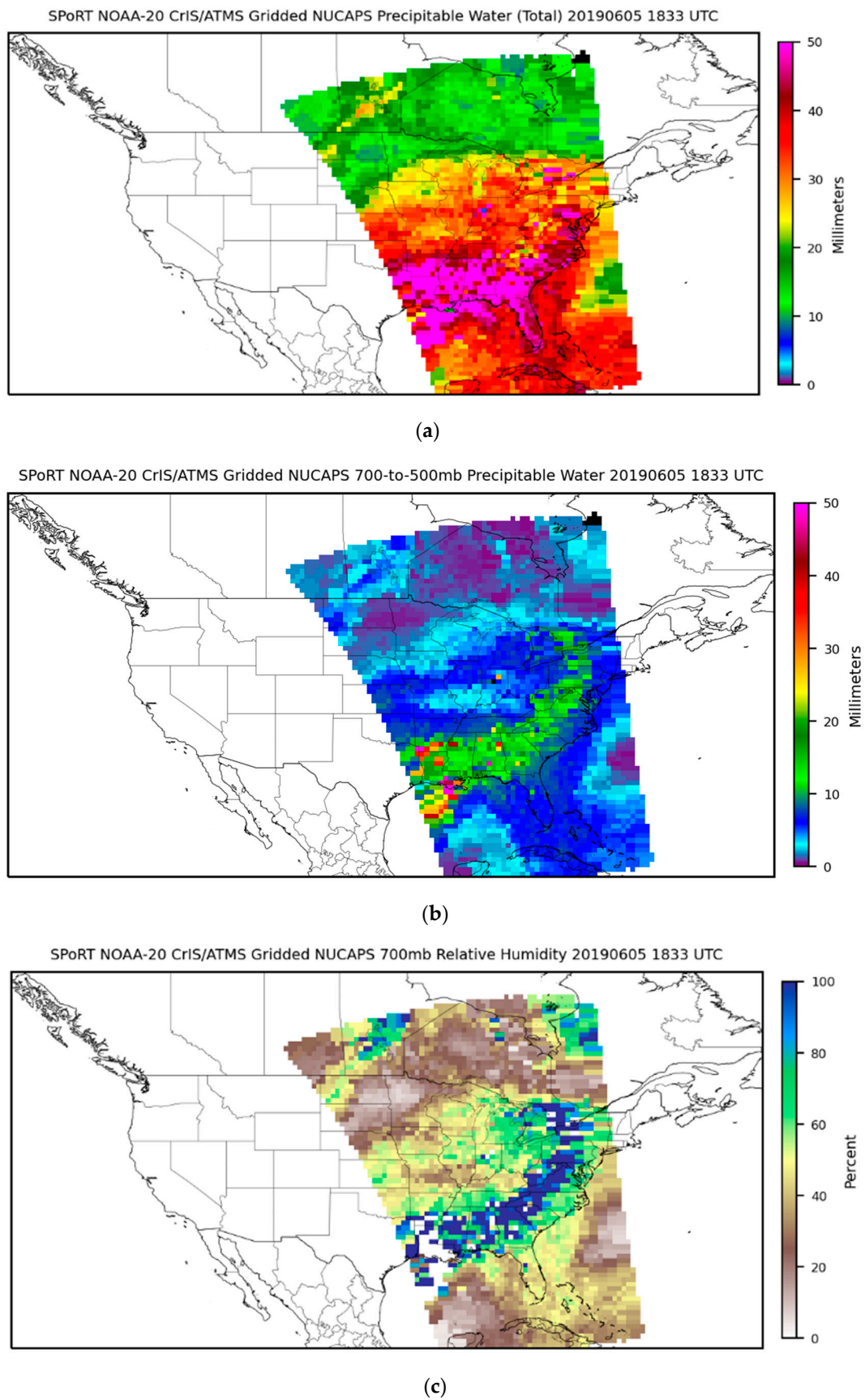


Figure 4. NOAA-20 Gridded NUCAPS on 5 June 2020, 1833 UTC (a) total precipitable water (TPW), (b) 700–500 hPa layer precipitable water (LPW), and (c) 700 hPa relative humidity.

3.2. Fire Weather Analysis

Fire weather is an emerging application to utilize NUCAPS soundings and gridded products to diagnose the thermodynamic characteristics of the environment conducive to the potential for wildfire development and growth, as well as tracking smoke [46,47]. Lindley et al. [48] provide an overview of the common meteorological features associated with wildfires in the southern Great Plains, notably the development of low-level thermal ridges (LLTR). The example presented below highlights the ability of Gridded NUCAPS products to capture the LLTR associated with the 2018 Rhea, Oklahoma fire. In addition, the derived parameters in AWIPS allow for the derivation of the Haines Index.

The Rheafire started around 12 April 2018 and burned approximately 285,196 acres [49]. The region was experiencing an extreme drought and on this particular day a dry line was positioned to the east and an LLTR developed. Lindley et al. [48] suggest the analysis of fields such as mean sea level pressure, 2-meter temperature and relative humidity, 850 hPa temperature, and 500 hPa height to identify the LLTR. Gridded NUCAPS fields from both the S-NPP 1845 and 2025 UTC overpasses can be combined and compared to the 2000 UTC Rapid Update (RAP) model data (Figure 5). The level of 700 hPa was chosen to view data above the influence of topography, as some missing values were apparent at 850 hPa over the Rocky Mountains, impeding broad synoptic analysis. The 2 m temperature and relative humidity fields from NUCAPS indicate warm (25–30 °C temperatures) and dry (10–20% relative humidity) conditions in western Oklahoma (Figure 5a,b). The 10 m RAP winds indicate that these warm, dry conditions are being advected into the region. Analysis of the 700 hPa temperature field indicates the thermal ridge axis over the region (Figure 5c). This feature identified in the Gridded NUCAPS is consistent with the RAP model (Figure 5d), and the RAP 500 hPa height is consistent with the expected pattern of an LLTR.

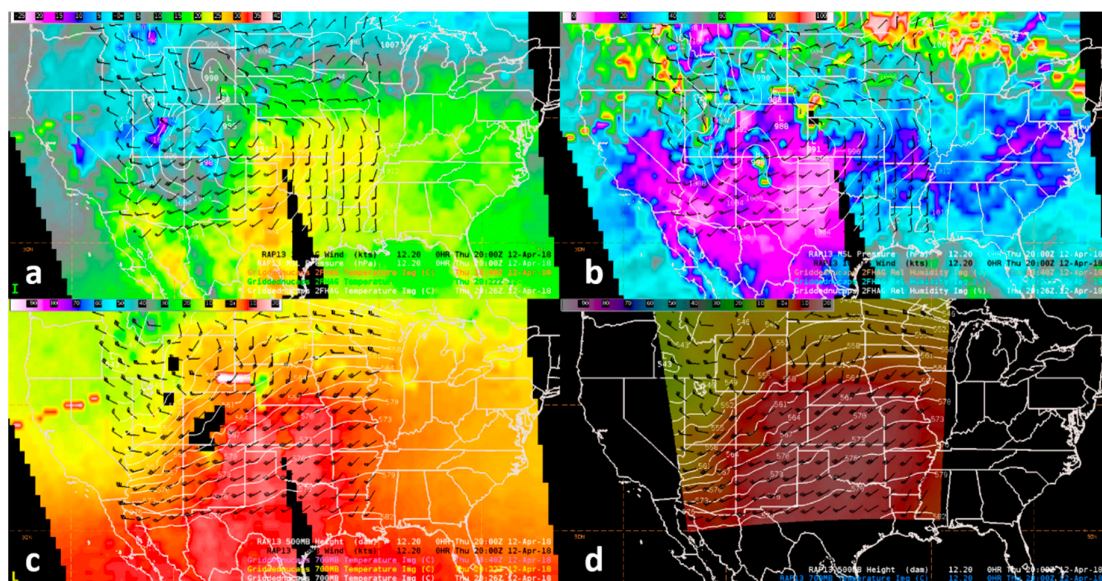


Figure 5. Advanced Weather Interactive Processing System (AWIPS) display of the 12 April 2018 Suomi-National Polar-orbiting Partnership (S-NPP) Gridded NUCAPS 1839 and 2021 UTC overpass and Rapid Update (RAP) model 2000 UTC analysis. (a) Gridded NUCAPS 2 m temperature, RAP surface wind, and mean sea level pressure; (b) Gridded NUCAPS 2 m relative humidity, RAP surface wind, and mean sea level pressure; (c) Gridded NUCAPS 700 hPa temperature and RAP 500 hPa wind and height; (d) RAP 700 hPa temperature, 500 hPa wind and height. Note that the AWIPS regional localization prevents the display of RAP on a full conus domain.

On 13 April, these same features continued to persist. The surface thermodynamic fields (Figure 6a,b) reveal the continued persistence of warm, dry conditions, and the well-defined LLTR visually agrees with the RAP analysis (Figure 6c,d). In addition, the Gridded NUCAPS Haines Index

did indicate a broad region (orange) of high potential for large fire growth, consistent with the RAP analysis. The Haines Index, calculated with the 850–700 hPa lapse rates and 850 hPa dew point depression, depicted a region of high potential for fire growth over western Oklahoma, but with an axis shifted to the east compared to the RAP model (Figure 7a,b). The Gridded NUCAPS thermodynamic fields and the derived Haines Index demonstrate the application of Gridded NUCAPS to increase the situational awareness of fire weather conditions and the potential for fire growth. The combination of Gridded NUCAPS fields, supplemented by additional model fields such as wind and height, are demonstrated as a viable dataset for the identification of an LLTR. The Gridded NUCAPS fields can provide observations between model runs and are a model-independent observational dataset to confirm model features such as patterns and gradients.

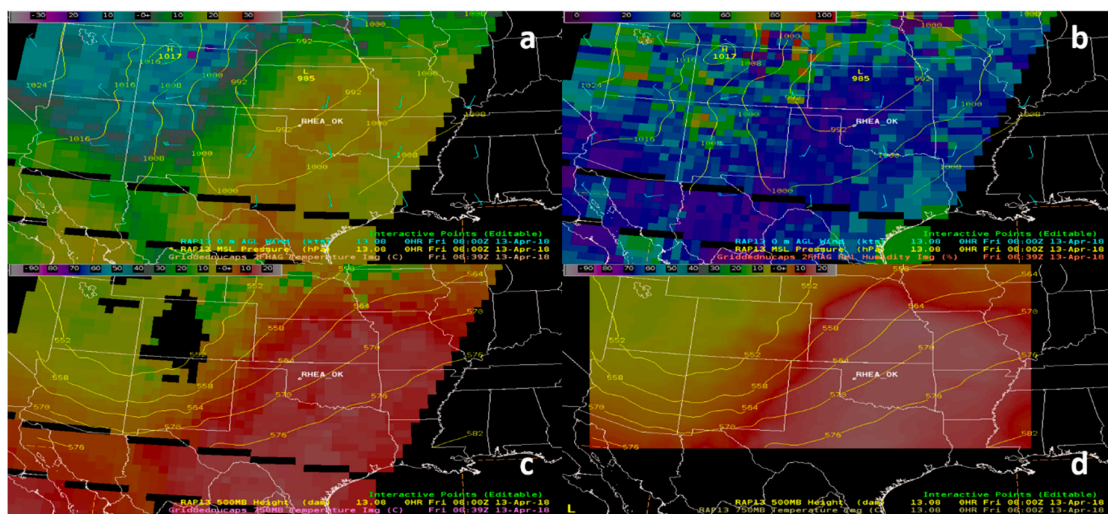


Figure 6. AWIPS display of 13 April 2018 S-NPP Gridded NUCAPS 0839 UTC overpass and RAP 0800 UTC analysis. (a) Gridded NUCAPS 2 m temperature, RAP surface wind, and mean sea level pressure; (b) Gridded NUCAPS 2 m relative humidity, RAP surface wind, and mean sea level pressure; (c) Gridded NUCAPS 750 hPa temperature and RAP 500 hPa height; (d) RAP 750 hPa temperature and 500 hPa height.

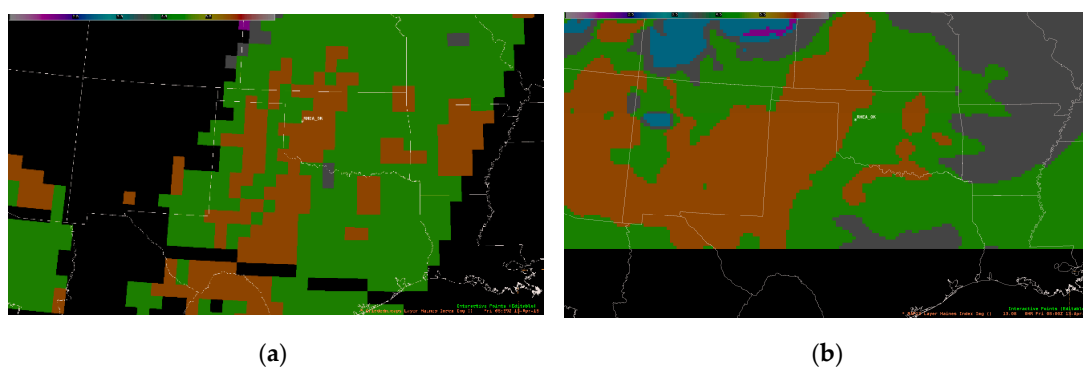


Figure 7. AWIPS display of Haines Index calculated from the 850–700 hPa lapse rate and 850 hPa dew point depression. (a) S-NPP Gridded NUCAPS Haines Index for 13 April 2019 0839 UTC overpass and (b) RAP Haines Index for the 13 April 0800 UTC analysis.

3.3. Monitoring the Saharan Air Layer

The NUCAPS retrievals perform well in clear to partly cloudy conditions; therefore, the Saharan Air Layer (SAL) is an ideal atmospheric phenomenon to observe and monitor. The SAL is an air mass of warm, dry, and often very dusty conditions that originates within the Saharan deserts in northern Africa, then propagates westward for several thousand kilometers, depending on its strength and

favorable surrounding environments [50,51]. Using true color imagery, the SAL is identified as a distinct brown (dusty) plume propagating off the northwest coast of Africa, as shown in Figure 8.



Figure 8. NOAA-20 Visible Infrared Imaging Radiometer Suite (VIIRS) True Color imagery on June 22 obtained from NASA Worldview (<https://worldview.earthdata.nasa.gov/>). The brownish plume that covers the Dominican Republic, Puerto Rico, and the West Indies reveals a strong dust presence associated with the SAL in this region. The bright white rectangular feature toward the top middle portion of the image is sun glint.

From a thermodynamic perspective, [52] used available land-based rawinsonde measurements to provide Skew-T Log P profiles to track the lifespan of a typical SAL outbreak. Near the source region, the SAL outbreak is initially featured with a constant theta (dry adiabatic) profile from the surface to some elevated level, approximately 500 hPa. The accompanying mixing ratio profile starts as very dry at the surface, leading up to 500 hPa to cap the upper extent of the SAL. As the feature propagates westward over the eastern Atlantic basin just offshore of northwest Africa, the surface becomes cut off from the cool and moist marine boundary layer. Finally, the SAL layer greatly becomes diluted by the surrounding cumulus cloud fields and mixing with the boundary layer as it encounters the greater Caribbean and western Atlantic region. Dunion and Marron [53] showed how the mixing ratio at 700 mb is marked by a dry anomaly during a SAL event as compared to the nominal occurrence of the moist tropical environment. The SAL is also accompanied with a low level easterly jet (<10,000 ft). As a result, the slate of NUCAPS sounding products can greatly aid forecasters and analysts in the identification of the SAL, particularly over the data-sparse open water of the Atlantic [54]. The identification of this feature is not only important for impacting hurricane development or suppression [55], but also contributes to adverse health impacts [51,56].

Frequent summertime SAL outbreaks can occur during mid-June through to late August and are of great concern to forecasters and public health agencies throughout the greater Caribbean. Specifically, the population situated within the Caribbean islands, northern South America, the Gulf of Mexico, and the southern United States are particularly impacted by high aerosol content, leading to health hazards associated with poor air quality, as dust concentrations often exceed the United States Environmental Protection Agency standards for PM 2.5 and PM 10. Previous studies [51,56] report that the SAL-related airborne dust impacts Puerto Ricans and its neighboring islands throughout the West Indies, as they suffer from some of the worst global asthma rates, far greater than those of the mainland United States. These results translate into more frequent medical visits and higher mortality rates, especially among the very young and elderly. As the SAL progresses farther west, the feature becomes more diffuse

and the satellite identification becomes harder to identify, as the SAL typically encounters cumulus clouds and maritime mixing. The NWS WFO in San Juan, Puerto Rico, monitors and predicts the strength and progression of the SAL in order to issue accurate and timely warnings, and is constantly interested in new environmental resources to improve the accuracy and timeliness of significant SAL event predictions. One of the most sought-after analysis tools is atmospheric soundings, which are greatly lacking in the upstream and data-sparse Atlantic basin. It is here that the NUCAPS Skew-T soundings and gridded formats are currently being investigated.

One of the best opportunities in exploiting the thermodynamic characteristics of the “classic SAL” occurred during the period 17–29 June 2020, where satellite, model, and surface-based measurements highlighted very strong SAL signatures throughout its progression. This episode became a noteworthy global media concern, as human impacts from the Saharan dust were considered an exacerbation of the novel coronavirus pandemic, particularly over the greater Caribbean and southern United States populations. The NOAA-20 Visible Infrared Imaging Radiometer Suite (VIIRS) true color imagery (Figure 8) was used to track the dust plume from its source over northwest Africa through the tropical north Atlantic basin. Note the fairly cloud-free region within the associated dust pattern, which is quite unusual this far from the source region. The strength of the SAL is dramatized as far downwind as off the southeast United States coast on 28 June. Figure 9 provides a mapping of the approximate SAL positions for each day. The “X” within each dot are days that have corresponding plots, as displayed in Figure 10. In Figure 10, the profiles for June 21 and 23 are very similar to a typical SAL event, with the temperature (solid red) lines following constant theta, or dry adiabat from 900 hPa to ~650 hPa. Within the same depth, the mixing ratio profile (dashed red line) follows a slightly drier than constant w profile. The mixing ratio line reaches 600 hPa before reaching another dry layer above 500 hPa.

A number of Gridded NUCAPS products, as sampled in Figure 11, depict strong SAL signatures within each of the products. TPW (Figure 11a) and 700–500 hPa LPW (Figure 11b) exhibit lower precipitable water values in the vicinity of the SAL, as seen in the true color imagery (Figure 8). Although not shown, the near-surface LPW (sfc-850 hPa) indicates moist near-surface conditions, consistent with SAL characteristics. Additionally, warm conditions are evident in the 850 hPa temperature (Figure 11c) Gridded NUCAPS field. Fields such as relative humidity and lapse rate can additionally be analyzed to identify the SAL to further assess dry, stable conditions. Even the Gridded NUCAPS ozone anomaly indicates elevated ozone values in the SAL region, consistent with previous literature [57,58], where elevated ozone mixing ratio values were observed above the SAL. However, additional analysis is needed to determine the efficacy of utilizing the ozone anomaly for SAL identification. As demonstrated here and in other studies [54,59], the NUCAPS vertical soundings and Gridded NUCAPS present new opportunities to analyze the physical process and characteristics of the SAL as it traverses the data-sparse Atlantic basin.

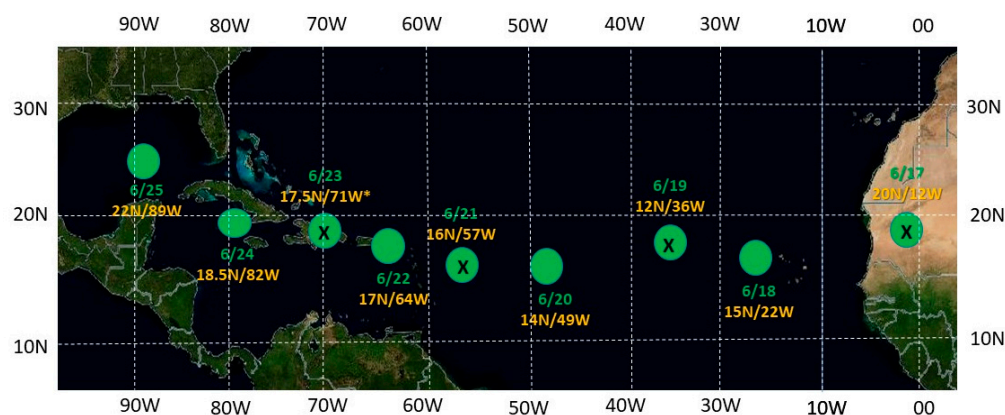


Figure 9. Map of approximate SAL positions (dots) for each afternoon during 17–25 June 2020. Circles with inner “X” annotations are related to the corresponding Skew-T Log P profiles in Figure 10 below.

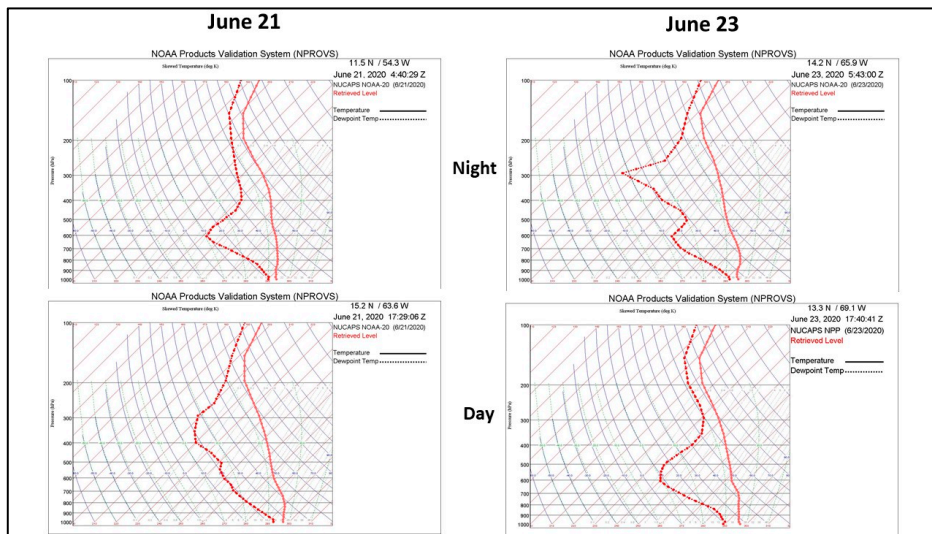


Figure 10. Composites of early morning (night) and afternoon (day) Skew-T plots of temperature (solid lines) and dew point temperature (dashed lines) of the S-NPP and NOAA-20 NUCAPS over the locations mapped in Figure 9 for June 21 and 23.

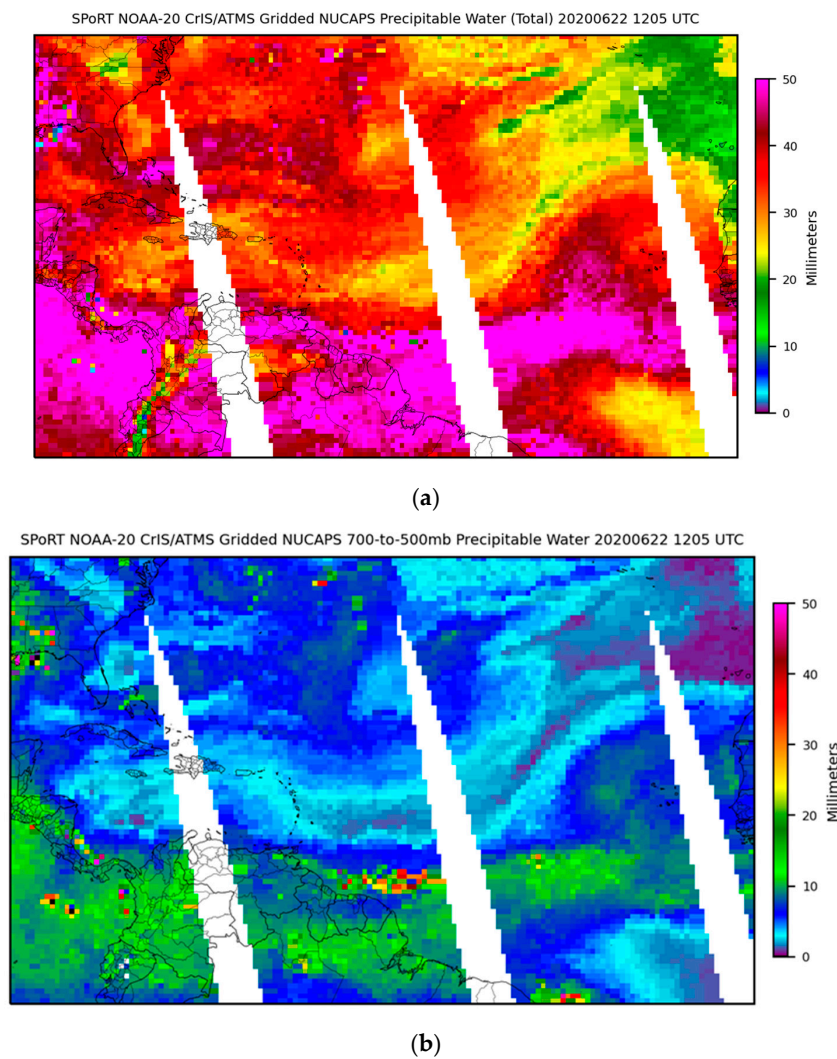


Figure 11. Cont.

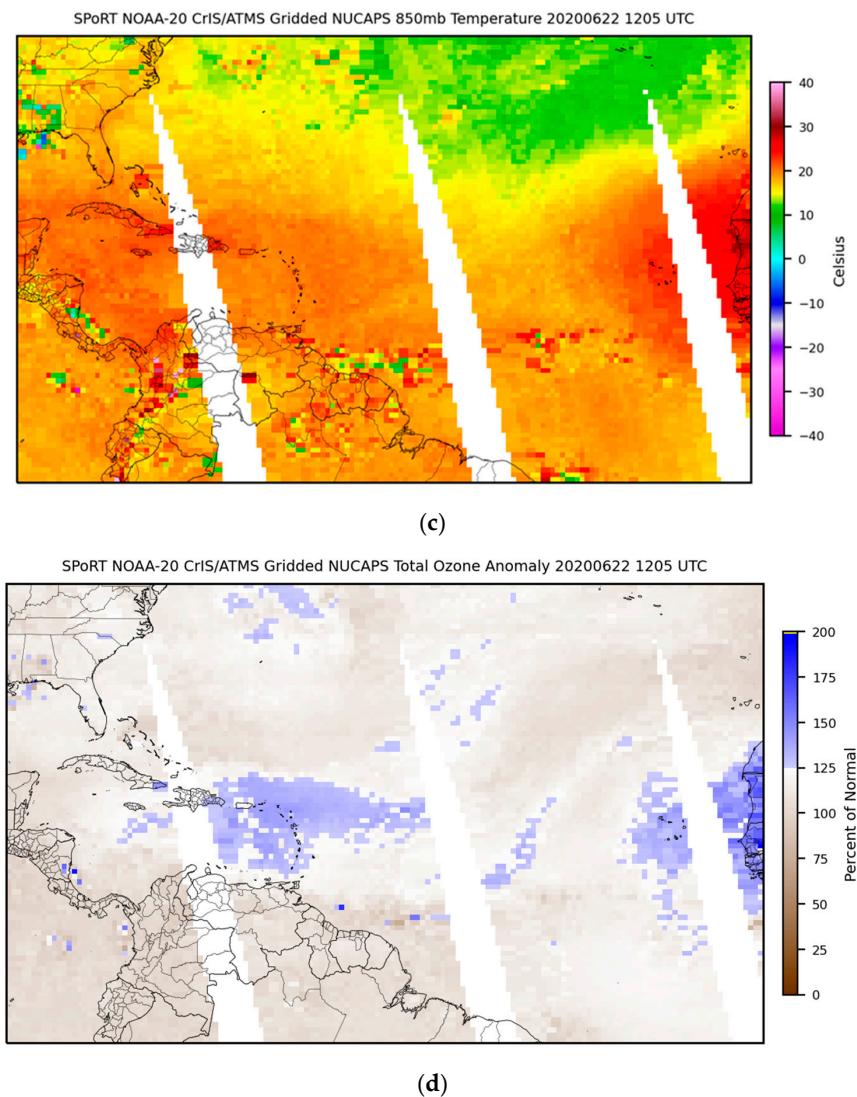
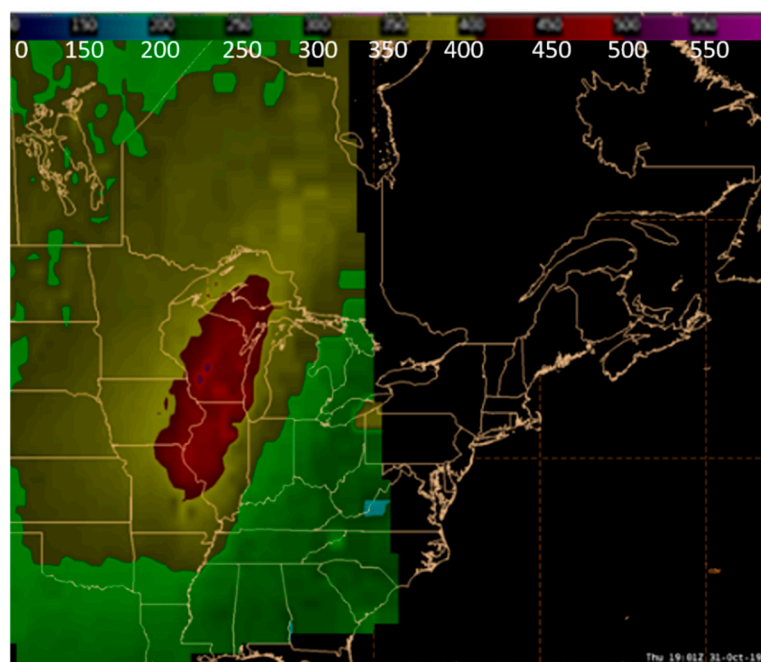


Figure 11. The 22 June 2020, 1205 to 1900 UTC NOAA-20 Gridded NUCAPS (a) TPW, (b) 700–500 hPa layer precipitable water, (c) 850 hPa temperature, and (d) ozone anomaly.

3.4. Identifying Stratospheric Air Influence and Tropopause Folding

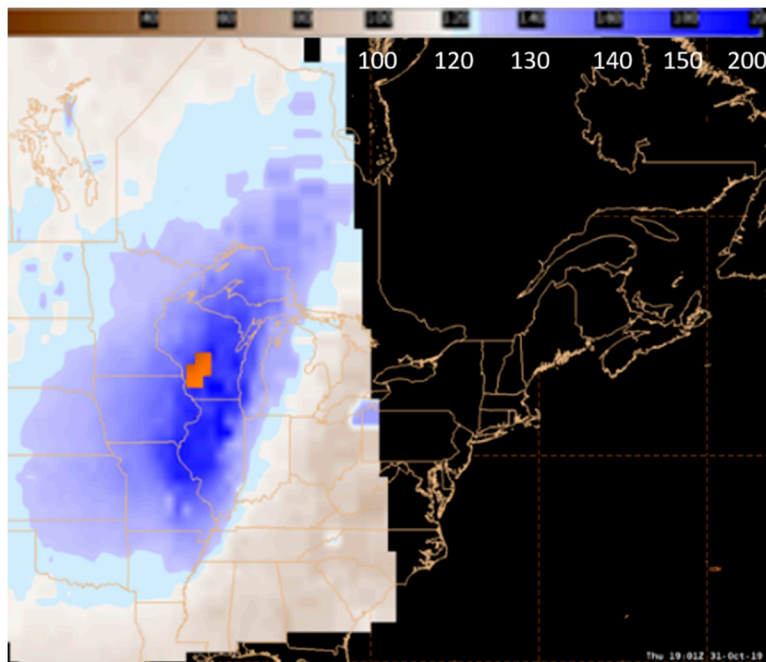
The Gridded NUCAPS ozone and ozone-derived products can be used to identify the influence of stratospheric air on weather systems and processes such as cyclogenesis, hurricane tropical to extratropical transition, and stratospherically-driven near surface high wind events, predicated on previous work by [19–21]. The ability to identify stratospheric air influence and the potential for tropopause folding can increase situational awareness of the development of hazards (damaging winds, high waves, and heavy rain) associated with these types of events. In addition, the identification of the tropopause can be an important indicator for the potential for turbulence in the vicinity of the jet stream due to the large gradients in temperature and wind [60]. Given the smooth nature of the NUCAPS vertical soundings, the identification of the tropopause features (e.g., isothermal layer and/or inversion) is not always straightforward. Since ozone is a precursor for stratospheric intrusions given the high ozone content of air above the tropopause [61,62], NUCAPS ozone and ozone-derived products can be utilized to identify stratospheric intrusions and the potential for tropopause folding. The example below highlights an instance where the evaluation of Gridded NUCAPS and radiosondes were used to diagnose the tropopause height.

A low-pressure system was traversing the Upper Midwest and Ohio Valley from 31 October to 1 November 2019 and deepening and maturing with time. Figure 12a shows an area of high ozone content associated with the passing cyclone. Since the total column ozone varies climatologically with season and latitude, high ozone values alone are a difficult metric for the identification of anomalous stratospheric air [21], associated with the descent of warm, dry ozone-rich air and its accumulation in the atmospheric column. Figure 12b indeed indicates that the region of high ozone values is associated with anomalous values of the total column ozone for the latitude and season. The darker blue values starting at 125% and greater represent the accumulation of stratospheric air and the potential for tropopause folding. The ozone-derived tropopause level (Figure 12c) indicates that the tropopause was as low as 550–650 hPa over western Illinois and 450–550 hPa over a broad region of the upper Midwest. Although the NOAA-20 overpass was around 1900 UTC on the 31 October, the analysis of the 0000 UTC 1 November sounding at Lincoln, Illinois, confirms a lower tropopause with a double tropopause signature observed at 500 and 300 hPa (Figure 13a). The difference between the Gridded NUCAPS and radiosonde could be explained by the comparison of differing observation types (e.g., points versus an area spanning 50km within the sounding footprint). The radiosonde at Green Bay, Wisconsin, indicates a higher tropopause at about 475 hPa, consistent with the Gridded NUCAPS product (Figure 13b). The comparison of the Gridded NUCAPS ozone-derived products to radiosondes here and in previous literature [19,21] demonstrates the value of ozone-derived fields for assessing the presence of stratospheric air and the potential for tropopause folding. The identification of these features in a plan-view perspective are important in applications such as forecasting rapid cyclogenesis and the development of high winds over data-sparse ocean basins, anticipating hurricane tropical to extratropical transition, and assessing the potential for turbulence near jet streams [63]. With Gridded NUCAPS in AWIPS, these fields are available for testing and demonstrating these applications.

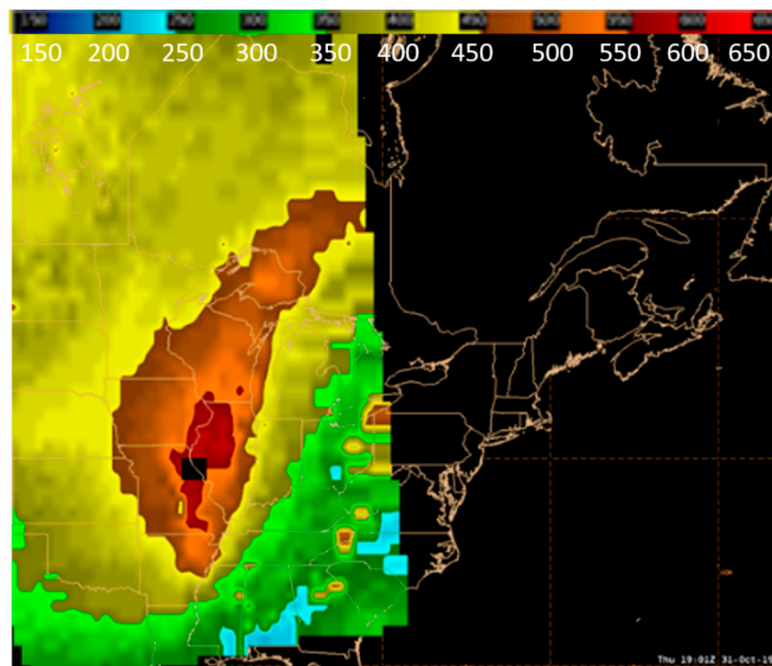


(a)

Figure 12. Cont.



(b)



(c)

Figure 12. AWIPS display of NOAA-20 Gridded NUCAPS on the 31 October 2019, 1901 UTC: (a) total column ozone, (b) ozone anomaly, and (c) tropopause level.

An example of the extratropical transition of Hurricane Arthur in 2014 highlights additional analysis that can increase the situational awareness of changes in the hurricane environment as it relates to anticipating changes in storm intensity. During 4 July, Arthur interacted with an upstream mid-latitude trough and accelerated northeastward. The warm, dry stratospheric air associated with the upper-level trough is colored orange in the air mass composite imagery (Figure 14a; [19,21,65–67]) derived from the Moderate Resolution Imaging Spectroradiometer onboard NASA’s Aqua satellite. Figure 14b shows that the stratospheric air is drawn further into the storm over the next 23 h. According to the National

Hurricane Center [68], Arthur began to lose strength as the storm encountered strong upper-level winds and colder sea-surface temperatures. Arthur was classified as a tropical storm by 0600 UTC on 5 July and deemed extratropical by 1200 UTC. Figure 14b is 5.5 h after the extratropical classification.

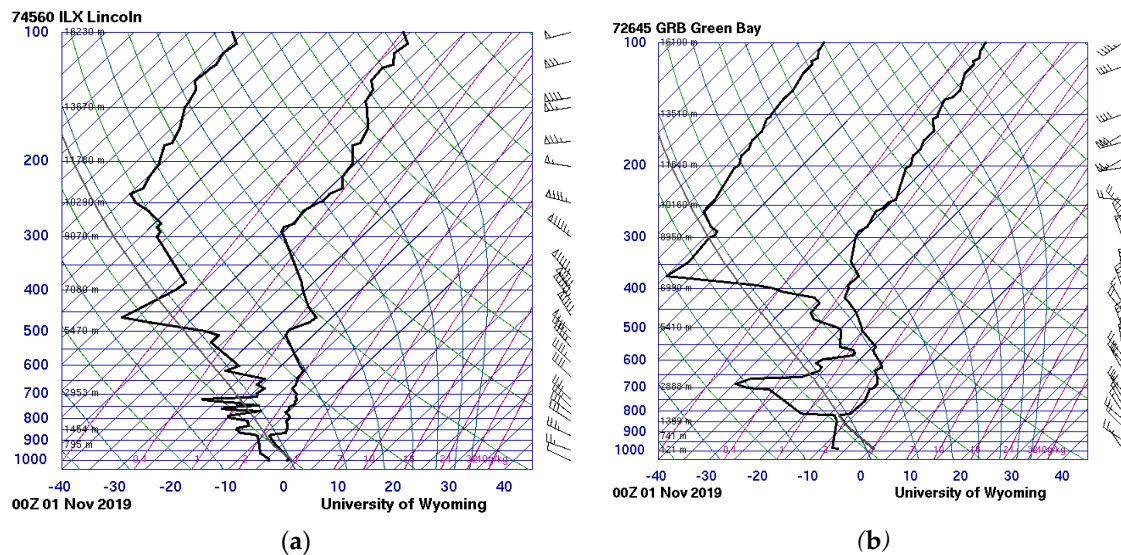


Figure 13. The 1 November 2019, 0000 UTC sounding at (a) Lincoln, Illinois, and (b) Green Bay, Wisconsin. Images retrieved from the University of Wyoming [64].

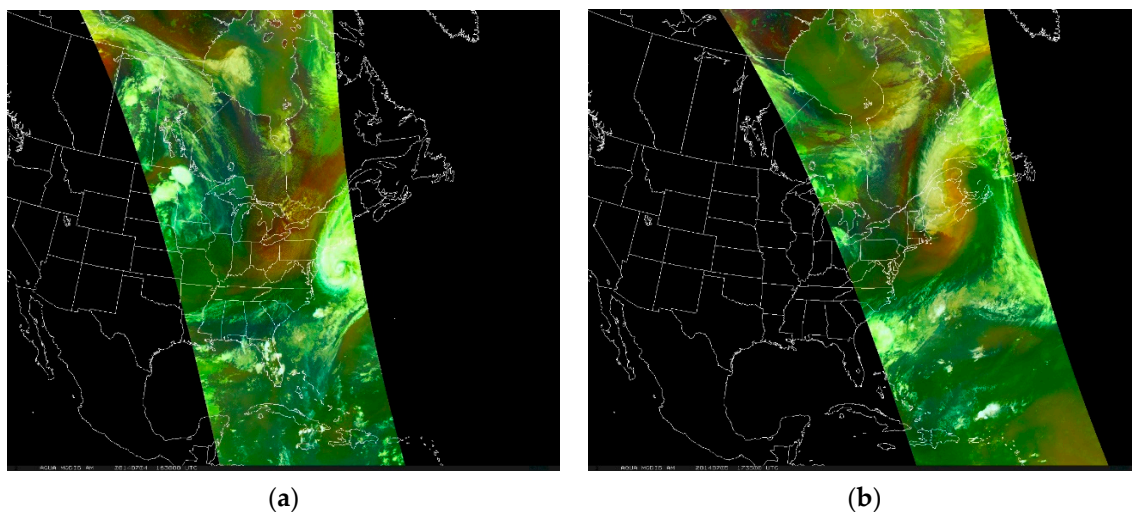


Figure 14. Aqua MODIS Air Mass Composite Imagery on (a) 4 July 2014 1835–1845 UTC and (b) 5 July 2014 1735–1750 UTC.

Building on the work of Berndt [69], which analyzes the S-NPP overpasses leading up to and following the extratropical transition of Arthur (2014), Gridded NUCAPS can provide additional insights into the hurricane environment and synoptic interactions. The upper-level trough can be identified in the Gridded NUCAPS 500-hPa temperature field, and dry 500 hPa conditions are present in the near-storm environment (Figure 15a,b). The interaction with the 500 hPa trough becomes more pronounced by 0605 UTC, and dry air is closer to the storm center (Figure 15c,d), increasing the situational awareness of the pending extratropical transition. This interaction is much more pronounced by 1735 UTC on 5 July (Figure 15e,f). The ozone anomaly and tropopause height fields can be analyzed to determine the potential for stratospheric intrusion and tropopause folding. The ozone anomaly indicates that a region of stratospheric air is present (Figure 16a; blue colors), but still west of

the storm center. In addition, low tropopause heights of 400–500 hPa are associated with this region (Figure 16b). Correspondence with model fields such as potential vorticity can confirm these features. By 0605 UTC on the 5 July, the region of stratospheric air and lower tropopause was much closer to the storm center (Figure 16c,d) and was further drawn into the storm by the afternoon (Figure 16e,f). Events such as extratropical transition and rapid cyclogenesis can create damaging winds, waves, and storm surges that can impact the populous region along the eastern United States or marine activities in the Atlantic and Pacific basins. Gridded NUCAPS, as another observational dataset, can support the thermodynamic and synoptic analysis of these events and complement model analyses to increase the situational awareness of changes in storm intensity that create hazardous conditions.

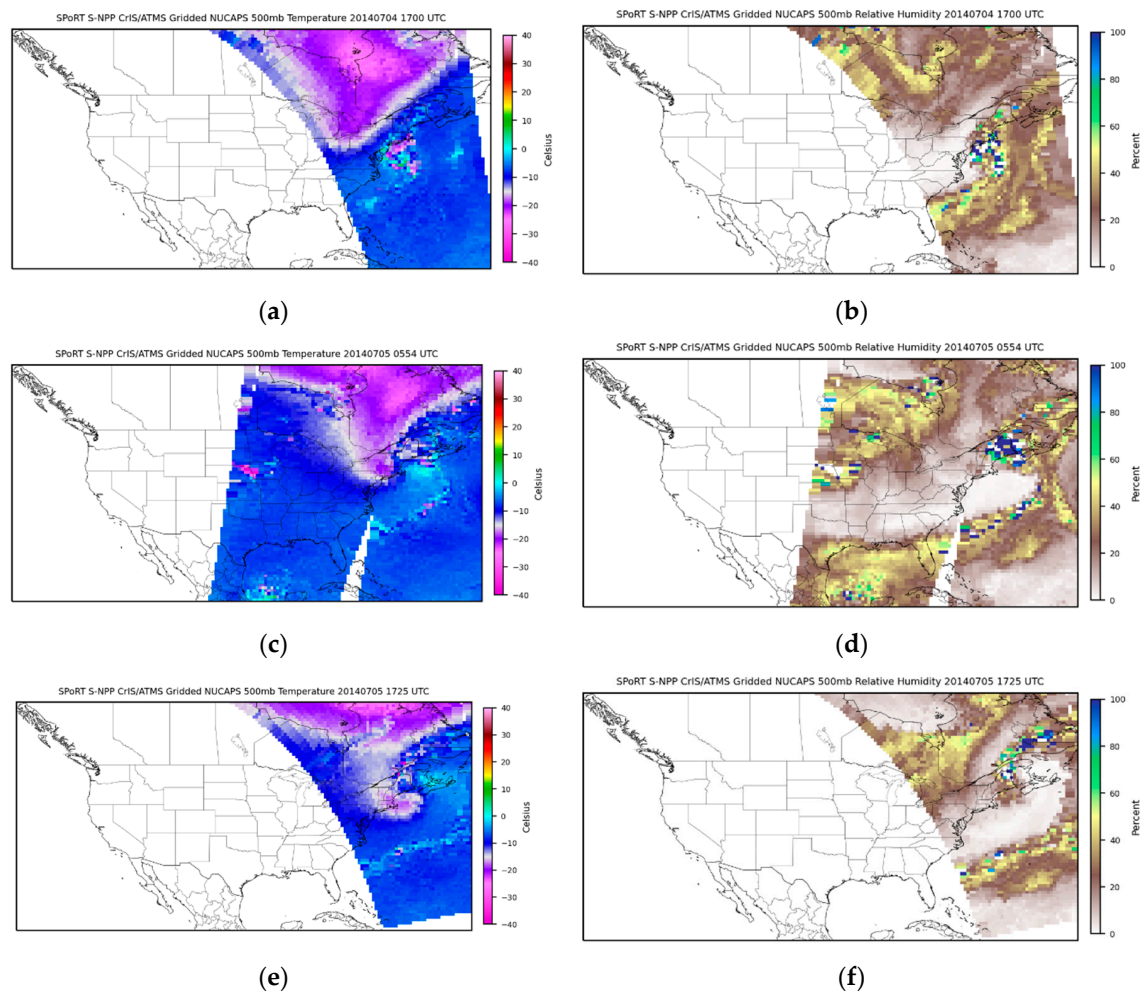


Figure 15. S-NPP Gridded NUCAPS 500 hPa temperature (left) and relative humidity (right): (a,b) overpass time on the 4 July 1745–1755 UTC; (c,d) combined overpasses on the 5 July with 0605–615 UTC on the right and 0745–0755 UTC on the left; (e,f) valid on the 5 July 2014 1725–1735 UTC.

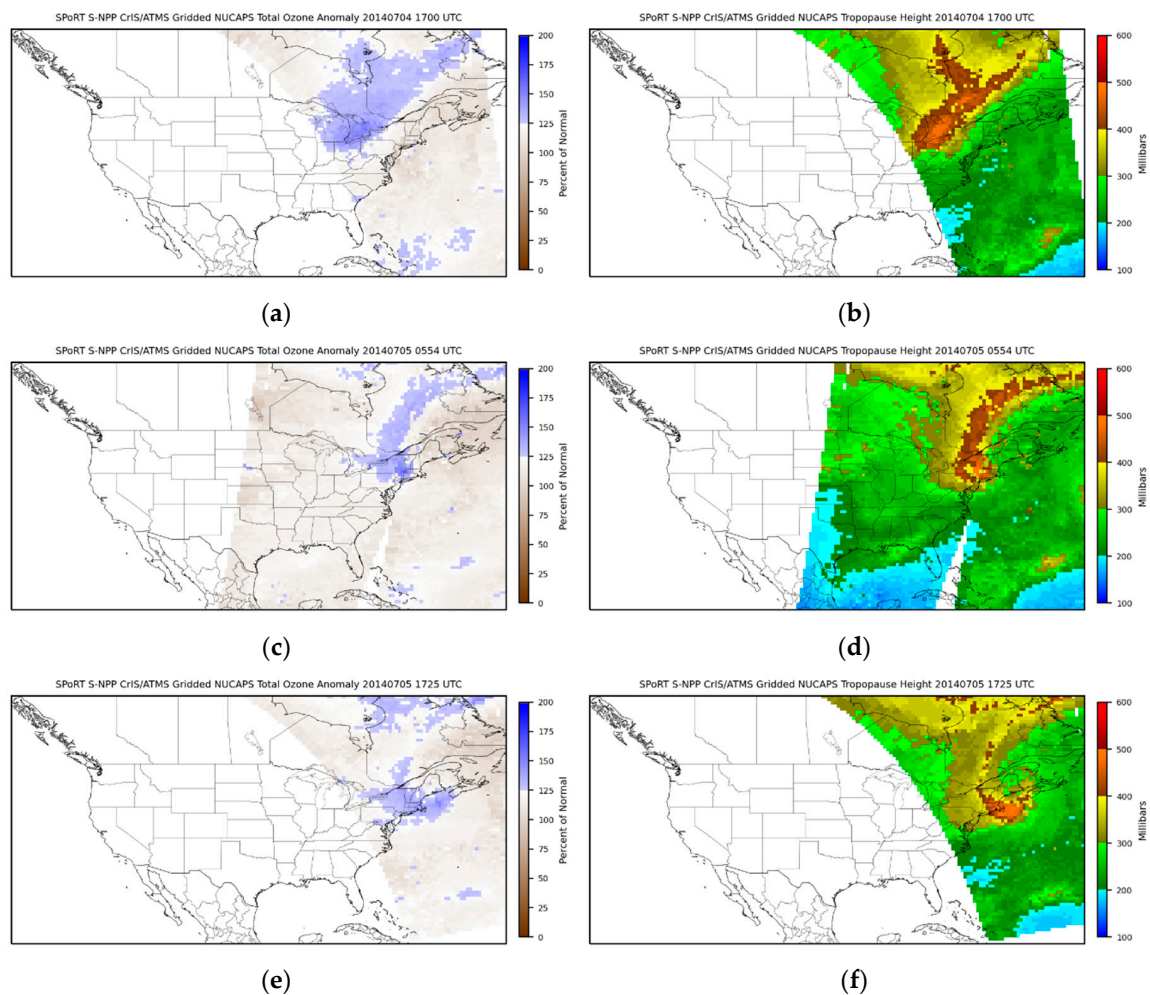


Figure 16. S-NPP Gridded NUCAPS ozone anomaly (left) and tropopause level (right): (a,b) overpass time on the 4 July 1745–1755 UTC; (c,d) combined overpasses on the 5 July with 0605–615 UTC on the right and 0745–0755 UTC on the left; (e,f) valid on the 5 July 2014 1725–1735 UTC.

4. Discussion

New methods and concepts and a standardized approach have been presented to create level 2 gridded and derived products from hyperspectral infrared sounding observations with a focus on NUCAPS observations and short-term weather forecasting. Traditional display tools such as skew-T diagrams, while important, do not fully exploit the strength of satellite soundings (personal communication, C. Barnett), and active user engagement with the weather community led to operations-to-research feedback, ultimately adapting NUCAPS to the operational environment [11]. The development of operationally relevant Gridded NUCAPS fields fills a gap, whereby NUCAPS level 2 gridded products to support short-term weather forecasting have been limited and now allow for the analysis of types of events suitable for thermodynamic analysis [47,63]. This method and capability advance the application and benefit of remote sensing observations, enabling novel analysis and the use of observations beyond their intended use. Few studies have presented methods to create level 2 gridded hyperspectral infrared products to support short-term weather forecasting, and the current structure of environmental data records as arrays of vertical soundings require additional data manipulation and processing. Although it is trivial for scientists to process and derive plan-view fields from hyperspectral infrared environmental data records through data processing and manipulation, this data structure has limited the use and application of hyperspectral soundings to the scientific community and advanced users. This work represents new, optimized processing to more

effectively visualize the information content of NUCAPS observations, making data more accessible to broader communities and allowing for information compression and the quick analysis of sounding observations [9]. The development of this level 2 gridding method and subsequent integration into baseline AWIPS for NWS-wide distribution was a direct result of operations-to-research feedback and the need to efficiently analyze many soundings in a short period of time, given the constraints, demands, and pace of the operational environment [11–13,17].

This work builds upon the early development of gridding dual-regression algorithm hyperspectral infrared soundings, where data were processed through the polar2grid software [5,29]. These early, experimental methods were adapted to NUCAPS observations in collaboration with the developers, as explained in [13], and further adapted for integration in AWIPS, as explained here. Experimental methods had to be adapted to conform with the constraints of the AWIPS system and available software without requiring burdensome computing expense or resources. The optimization of processing here to create level 2 gridded and derived products with the characteristics of the NUCAPS observations (e.g., footprint size, level vs. layer quantities, retaining data integrity) and the needs of end users in mind (e.g., compatibility with AWIPS, standard levels, fields of interest) represents a new method and technique for processing NUCAPS level 2 products and furthers the accessibility, value, and benefit of these observations to support a wide variety of science and applications. Although level 3 gridded products are routinely produced and available as standard NUCAPS products, there has been a gap in the development of level 2 products or standardized gridding approaches to support short-term weather forecasting. In addition, the derivation of more specialized fields beyond basic temperature, moisture, and trace gases have traditionally not been produced due to the lack of a standard approach to easily process level 2 products. As a feasibility study, [6] demonstrates the information content available to the operational weather community through the derivation of NUCAPS horizontal derived fields of stability indices for convective weather forecasting and emphasizes the advantages and limitations of NUCAPS for this application. The work described here presents the benefit of additional derived fields such as lapse rates, LPW, the Haines Index, and ozone products uniquely developed to optimize the benefit of ozone observations to identify and diagnose the dynamic processes that drive weather. The ozone anomaly and tropopause-level products are developed based on atmospheric dynamics principles relative to how the concentration of ozone varies over time and space as well as the relationship to dynamic variables such as potential vorticity. The processing and derivation of the TPW/LPW fields were designed to facilitate comparison with existing satellite-derived TPW/LPW products.

Few studies have defined or described a methodology for level 2 gridded hyperspectral infrared-derived products for short-term weather forecasting. Gridded NUCAPS products were the result of consciously listening and tailoring NUCAPS towards users' needs and represent a way for the forecaster to quickly assess the environment and highlight baroclinicity and other important features within our soundings to enable the acceptance and, more importantly, value of the NASA and NOAA satellite investments (personal communication, C. Barnett). As described here, this method developed through operations-to-research feedback represents a standard, reproducible approach to effectively visualize NUCAPS observations as level 2 gridded products for more effective analysis and interpretation. As this new approach is now available to all NWS forecasters in the operational AWIPS system and is available online through SPoRT (<https://weather.msfc.nasa.gov/cgi-bin/sportPublishData.pl?dataset=griddednucaps>), Gridded NUCAPS reaches a broader audience of applied science users for the assessment of novel applications.

5. Conclusions

Interaction with end users and product assessments within the context of the NASA SPoRT research-to-operations/operations-to-research paradigm [1] and collaboration within the NOAA JPSS PGRR Program Sounding Initiative have demonstrated the value of operations-to-research collaborations, specifically to provide insight into the limitations and advantages [11,13] of products to tailor them

for the operational environment. A new method and concept for the processing and representation of NUCAPS level 2 gridded and products is presented here, representing the development of approaches to better synthesize remote sensing observations that ultimately increase the availability and usability of NUCAPS observations to benefit scientific analysis and applications. The optimization of basic gridding and interpolation methodologies as appropriately applied to NUCAPS data retains observational characteristics and enables state-of-the-art product development to further support application in weather analysis and forecasting. The derived products presented herein represent the novel development of fields not traditionally derived from hyperspectral infrared sounder observations and new concepts/methods to support applications related to short-term weather forecasting and analysis. The early development and demonstration of Gridded NUCAPS for the cold air aloft aviation hazard and analysis of the pre-convective environment led to the development of a baseline National Weather Service (NWS) capability to create gridded displays of satellite sounding retrievals in the Advanced Weather Interactive Processing System (AWIPS). Gridded NUCAPS was released in AWIPS in 2019, enhancing the capabilities of NUCAPS temperature and moisture soundings that have been available to NWS forecasters as Skew-T's since 2014. The techniques described here were developed to optimally interpolate data to standard levels and grid observations on a 0.5° latitude/longitude grid with minimal interpolation. Each sounding is adjusted to account for changes in the local topography and surface pressure, removing data below the ground surface. Then, they are vertically interpolated to 41 standard meteorological levels from 1100 to 100 hPa every 25 hPa. Temperature is interpolated separately from water vapor and trace gases, which are converted from layer to level quantities and linearized by interpolating the standard logarithm of the column density. Each array of aggregated soundings is added to a 0.5° latitude/longitude grid over a global domain using nearest neighbor and minimal interpolation, masking regions outside of the swath prior to gridding. Horizontal fields are created for temperature and relative humidity on 41 standard levels and at the surface (e.g., 2 m); and derived single-layer products including: quality flags, total precipitable water (TPW) and layer precipitable water (LPW), total ozone, ozone anomaly, and tropopause level. The capabilities additionally include the derivation of lapse rates and the Haines Index. The development of operationally relevant Gridded NUCAPS fields allows for the analysis of types of events suitable to thermodynamic analysis [47,63] and fills a gap whereby NUCAPS level 2 gridded products for supporting short-term weather forecasting have been limited.

The examples presented here demonstrate the analysis possible with the new Gridded NUCAPS capability. Fields such as TPW, LPW, relative humidity, and lapse rates can be used to anticipate the development of convection, where the analysis of gradients and observations between model runs can increase situational awareness, which has already been demonstrated through assessments at the Hazardous Weather Testbed (HWT). The analysis of the 5 June 2019 case demonstrates the value of assessing the broad environment quickly through the identification of the moisture gradient along which the storm developed and produced strong winds. As an emerging application, the assessment of the fire weather environment with NUCAPS soundings is demonstrated here through the identification of the LLTR and analysis of the Haines Index. The near-surface and mid-level temperature and moisture fields were compared to model data to identify the synoptic pattern and LLTR that persisted on the 12–13 April and created weather conditions conducive to the development of the Rhea, Oklahoma fire in 2018. In addition, the derived Haines Index identified a region of high fire potential in the area. The combination of NUCAPS observations with additional model fields such as wind and height demonstrate the value of NUCAPS in supporting fire weather analysis as a model-independent observational dataset to identify thermodynamic features. The visualizations in AWIPS and through a website allow for NWS forecasters and Incident Meteorologists to use NUCAPS products during fire events such as the Rhea fire. Demonstrating the breadth of emerging applications, NUCAPS soundings and Gridded NUCAPS is shown as another observational dataset to identify the Saharan Air Layer (SAL). The June 2020 SAL event is analyzed with NUCAPS vertical profiles, capturing the dry layer on June 21 and 23 in the low to mid-levels. The Gridded NUCAPS TPW and LPW fields

were used in the identification of the spatial and vertical extent of the dry, dusty air layer, with the dry pronounced in the 700–500 hPa layer. In addition, elevated temperatures were observed in the NUCAPS 850 hPa temperature field in the SAL region, consistent with typical SAL conditions. Although warranting further analysis and investigation of the efficacy of the approach, an ozone anomaly product with values greater than 125% was observed in the SAL region; thus hinting at elevated ozone mixing ratios associated with the feature. Lastly, the ozone-derived products designed specifically for assessing changes in cyclone or hurricane intensity provide unique information for the identification of such events and anticipating hazards associated with stratospheric air and tropopause folding. The demonstration of the NUCAPS total column ozone, ozone anomaly, and tropopause level for identifying a double tropopause signature from 500 to 300 hPa in the upper Midwest from 31 October to 1 November 2019 captures the ability of Gridded NUCAPS to identify stratospheric intrusions and tropopause folding events. The additional analysis of the extratropical transition of Hurricane Arthur in 2014 was presented to demonstrate the capabilities of the Gridded NUCAPS temperature, moisture, and ozone fields. The Gridded NUCAPS 500 hPa temperature was used to track the development of the upper-level trough and interaction with the storm from 4 to 5 July. The interaction of dry air with the storm, one indicator of many for extratropical transition, was pronounced in the 500 hPa relative humidity fields with dry air infiltrating the storm center by 1735 UTC 5 July, shortly after the extratropical classification. The ozone anomaly and tropopause-level fields observed the region of stratospheric air and lower tropopause heights (400–500 hPa) associated with the upper-level trough, positioned west of the storm on 4 July, moving eastward, and interacting with the storm center by the afternoon of 5 July. Although these fields and applications were previously demonstrated related to the NOAA NWS Ocean Prediction Center analysis of deepening cyclones [19,21] and preliminarily introduced to the NOAA NWS National Hurricane Center [69], these fields are now more widely available to all NWS forecasters to apply to a broader set of applications [63]. The identification of the tropopause and jet stream interactions is important for anticipating changes in storm and hurricane intensity as well as turbulence.

As Gridded NUCAPS is under continued development to add additional derived products and improve the representation of soundings, such as accounting for surface and topography, there are opportunities to discover new applications and how the data can be used for scientific process studies. Additional fields such as trace gases can be processed for display in non-AWIPS visualizations to support additional end users related to tracking smoke plumes important to NWS Incident Meteorologists or researchers conducting field campaigns [46]. Although NUCAPS performs best in clear to partly cloudy conditions, the gridded fields derived from microwave-only soundings have the potential for utility for applications under non-precipitating, cloudy conditions where the microwave retrieval was still successful, such as aviation icing or evaluating the expected precipitation type [70]. There are opportunities to uncover new applications, such as the analysis of the hurricane environment [71,72] and understanding the processes related to the tropical cyclone diurnal cycle [73]. In addition, NUCAPS, especially with multi-satellite assessments and the use of microwave-only soundings, has potential as a proxy to demonstrate the capabilities of the upcoming NASA Time-Resolved Observations of Precipitation structure and storm Intensity with a Constellation of Smallsats (TROPICS; [74]) Mission as a dataset to prepare users for the analysis possible with this new mission. Lastly, the use of multiple satellite platforms or trajectory modeling [17,75] can increase the temporal and spatial coverage of observations, providing insight into the utility of a geostationary hyperspectral infrared sounder in the future.

Author Contributions: Conceptualization, E.B., N.S. and R.E.; software, J.B., N.S., E.B., F.L., J.S. and R.A.; investigation, E.B., K.W., R.A., A.K. and E.D.; resources, J.B., N.S., E.B., R.E., K.W., A.K., E.D., F.L., R.A., J.S.; writing, E.B., R.E., N.S., K.W., A.K., E.D., J.S.; visualization, J.B., E.B., N.S., A.K., F.L., J.S., R.E. and R.A.; supervision, E.B.; project administration, E.B.; funding acquisition, E.B., J.B., N.S., R.E.B. All authors have read and agreed to the published version of the manuscript.

Funding: This research was funded by Mitchell Goldberg through the Joint Polar Satellite System Proving Ground and Risk Reduction Program under the following projects: “The Cold Air Aloft Aviation Hazard: Detection Using Observations from JPSS Satellites and Applications to the Visualization of Gridded Soundings in AWIPS II”, “Expanded Application and Demonstration of Gridded NUCAPS in AWIPS”, and “NUCAPS Visualization”. In addition, this work was partially supported by Tsengdar Lee of the Earth Science Division at NASA Headquarters as part of the NASA Short-term Prediction Research and Transition Center at Marshall Space Flight Center.

Acknowledgments: The authors would like to thank the Joint Polar Satellite System Proving Ground Sounding Initiative for continued support and collaboration. The authors appreciate Christopher Barnet’s continual insights and discussions about the complexities of the NUCAPS algorithm. The authors also thank the National Weather Service end users who have participated in assessments and the NUCAPS Users Working Group to give operations-to-research feedback that has improved the products described herein.

Conflicts of Interest: The authors declare no conflict of interest.

References

- Jedlovec, G. Transitioning Research Satellite Data to the Operational Weather Community: The SPoRT Paradigm [Organization Profiles]. *IEEE Geosci. Remote Sens. Mag.* **2013**, *1*, 62–66. [[CrossRef](#)]
- Nalli, N.R.; Gambacorta, A.; Liu, Q.; Barnet, C.D.; Tan, C.; Iturbide-Sanchez, F.; Reale, T.; Sun, B.; Wilson, M.; Borg, L.; et al. Validation of Atmospheric Profile Retrievals From the SNPP NOAA-Unique Combined Atmospheric Processing System. Part 1: Temperature and Moisture. *IEEE Trans. Geosci. Remote Sens.* **2018**, *56*, 180–190. [[CrossRef](#)]
- Nalli, N.R.; Gambacorta, A.; Liu, Q.; Tan, C.; Iturbide-Sanchez, F.; Barnet, C.D.; Joseph, E.; Morris, V.R.; Oyola, M.; Smith, J.W. Validation of Atmospheric Profile Retrievals from the SNPP NOAA-Unique Combined Atmospheric Processing System. Part 2: Ozone. *IEEE Trans. Geosci. Remote Sens.* **2018**, *56*, 598–607. [[CrossRef](#)]
- Gambacorta, A.; Barnet, C.D. Methodology and Information Content of the NOAA NESDIS Operational Channel Selection for the Cross-Track Infrared Sounder (CrIS). *IEEE Trans. Geosci. Remote Sens.* **2013**, *51*, 3207–3216. [[CrossRef](#)]
- Weisz, E.; Smith, N.; Smith, W.L. The Use of Hyperspectral Sounding Information To Monitor Atmospheric Tendencies Leading to Severe Local Storms: HYPERSPECTRAL SOUNDERS TO MONITOR STORMS. *Earth Space Sci.* **2015**, *2*, 369–377. [[CrossRef](#)]
- Iturbide-Sanchez, F.; da Silva, S.R.S.; Liu, Q.; Pryor, K.L.; Pettey, M.E.; Nalli, N.R. Toward the Operational Weather Forecasting Application of Atmospheric Stability Products Derived From NUCAPS CrIS/ATMS Soundings. *IEEE Trans. Geosci. Remote Sens.* **2018**, *56*, 4522–4545. [[CrossRef](#)]
- Susskind, J.; Barnet, C.D.; Blaisdell, J.M. Retrieval of Atmospheric and Surface Parameters from AIRS/AMSU/HSB data in the Presence of Clouds. *IEEE TGRS* **2003**, *41*, 390–409. [[CrossRef](#)]
- Wheeler, A.; Smith, N.; Gambacorta, A.; Barnet, C.D. Evaluation of NUCAPS Products in AWIPS-II: Results from the 2017 HWT. In Proceedings of the 98th American Meteorological Society Annual Meeting, Austin, TX, USA, 7–11 January 2018.
- Smith, N.; White, K.D.; Berndt, E.B.; Zavodsky, B.T.; Wheeler, A.; Bowlan, M.A.; Barnet, C.D. NUCAPS in AWIPS—Rethinking Information Compression and Distribution for Fast Decision Making. In Proceedings of the 98th American Meteorological Society Annual Meeting, Austin, TX, USA, 7–11 January 2018.
- Ackerman, S.A.; Platnick, S.; Bhartia, P.K.; Duncan, B.; L’Ecuyer, T.; Heidinger, A.; Skofronick-Jackson, G.; Loeb, N.; Schmit, T.; Smith, N. Satellites See the World’s Atmosphere. *Meteorol. Monogr.* **2018**, *59*, 4.1–4.53. [[CrossRef](#)]
- Esmaili, R.B.; Smith, N.; Berndt, E.B.; Dostalek, J.F.; Kahn, B.H.; White, K.; Barnet, C.D.; Sjoberg, W.; Goldberg, M. Adapting Satellite Soundings for Operational Forecasting within the Hazardous Weather Testbed. *Remote Sens.* **2020**, *12*, 886. [[CrossRef](#)]
- Smith, N.; Berndt, E.B.; Barnet, C.D.; Goldberg, M.D. Why operational meteorologists need more satellite soundings. In Proceedings of the 99th American Meteorological Society Annual Meeting, Phoenix, AZ, USA, 6–10 January 2019.
- Weaver, G.; Smith, N.; Berndt, E.B.; White, K.D.; Dostalek, J.F.; Zavodsky, B.T. Addressing the Cold Air Aloft Aviation Challenge with Satellite Sounding Observations. *J. Oper. Meteorol.* **2019**, 138–152. [[CrossRef](#)]

14. Zavodsky, B.T.; Smith, N.; Dostalek, J.F.; Stevens, E.; Nelson, K.; Weisz, E.; Berndt, E.B.; Line, W.; Barnet, C.D.; Gambacorta, A.; et al. Development and Evaluation of a Gridded CrIS/ATMS Visualization for Operational Forecasting. In Proceedings of the 2016 AGU Fall Meeting, San Francisco, CA, USA, 12–16 December 2016. IN31A–1734.
15. Berndt, E.B.; Smith, N.; White, K.D.; Zavodsky, B.T. Development and Application of Gridded NUCAPS for Operational Forecasting Challenges. In Proceedings of the JPSS Science Seminar Series, Lantham, MD, USA, 23 October 2017.
16. Berndt, E.B. The Evolution of Gridded NUCAPS: Transition of Research to Operations. In Proceedings of the 99th American Meteorological Society Annual Meeting, Phoenix, AZ, USA, 6–10 January 2019.
17. Berndt, E.B.; Smith, N.; Burks, J.; White, K.D.; Allen, R.E. The Evolution of Gridded NUCAPS: Transition of Research to Operations. In Proceedings of the 2019 Joint Satellite Conference, Boston, MA, USA, 28 September–4 October 2019.
18. Ralph, F.M.; Intrieri, J.; Andra, D.; Atlas, R.; Boukabara, S.; Bright, D.; Davidson, P.; Entwistle, B.; Gaynor, J.; Goodman, S.; et al. The Emergence of Weather-Related Test Beds Linking Research and Forecasting Operations. *Bull. Am. Meteorol. Soc.* **2013**, *94*, 1187–1211. [[CrossRef](#)]
19. Zavodsky, B.; Molthan, A.; Folmer, M. Multispectral Imagery for Detecting Stratospheric Air Intrusions Associated with Mid-Latitude Cyclones. *J. Oper. Meteorol.* **2013**, *1*, 71–83. [[CrossRef](#)]
20. Berndt, E.; Folmer, M. Utility of CrIS/ATMS Profiles to Diagnose Extratropical Transition. *Results Phys.* **2018**, *8*, 184–185. [[CrossRef](#)]
21. Berndt, E.B.; Zavodsky, B.T.; Folmer, M.J. Development and Application of Atmospheric Infrared Sounder Ozone Retrieval Products for Operational Meteorology. *IEEE Trans. Geosci. Remote Sens.* **2016**, *54*, 958–967. [[CrossRef](#)]
22. Rodgers, C.D. *Inverse Methods for Atmospheric Sounding: Theory and Practice*; Series on Atmospheric, Oceanic and Planetary Physics—Vol. 2; World Scientific Publishing Co.: Singapore, 2000; pp. 1–243. ISBN 978-981-02-2740-1.
23. Irion, F.W.; Kahn, B.H.; Schreier, M.M.; Fetzer, E.J.; Fishbein, E.; Fu, D.; Kalmus, P.; Wilson, R.C.; Wong, S.; Yue, Q. Single-Footprint Retrievals of Temperature, Water Vapor and Cloud Properties from AIRS. *Atmos. Meas. Tech.* **2018**, *11*, 971–995. [[CrossRef](#)]
24. Smith, N.; Barnet, C.D. CLIMCAPS Observing Capability for Temperature, Moisture and Trace Gases from AIRS/AMSU and CrIS/ATMS. *Atmos. Meas. Tech. Discuss.* **2020**. [[CrossRef](#)]
25. Rosenkranz, P.W. Retrieval of Temperature and Moisture Profiles from AMSU-A and AMSU-B Measurements. *IEEE Trans. Geosci. Remote Sens.* **2001**, *39*, 2429–2435. [[CrossRef](#)]
26. Fu, D.; Bowman, K.W.; Worden, H.M.; Natraj, V.; Worden, J.R.; Yu, S.; Veeffkind, P.; Aben, I.; Landgraf, J.; Strow, L.; et al. High-Resolution Tropospheric Carbon Monoxide Profiles Retrieved from CrIS and TROPOMI. *Atmos. Meas. Tech.* **2016**, *9*, 2567–2579. [[CrossRef](#)]
27. Bowman, K.W.; Rodgers, C.D.; Kulawik, S.S.; Worden, J.; Sarkissian, E.; Osterman, G.; Steck, T.; Lou, M.; Eldering, A.; Shephard, M.; et al. Tropospheric Emission Spectrometer: Retrieval Method And Error Analysis. *IEEE Trans. Geosci. Remote Sens.* **2006**, *44*, 1297–1307. [[CrossRef](#)]
28. Goldberg, D.G.; Qu, Y.; McMillin, L.M.; Wolf, W.; Zhou, L.; Divakarla, G. AIRS Near-Real-Time Products and Algorithms in Support of Operational Numerical Weather Prediction. *IEEE TGRS* **2003**, *41*, 379–389. [[CrossRef](#)]
29. Smith, W.L.; Weisz, E.; Kireev, S.V.; Zhou, D.K.; Li, Z.; Borbas, E.E. Dual-Regression Retrieval Algorithm for Real-Time Processing of Satellite Ultraspectral Radiances. *JAMC* **2012**, *51*, 1455–1476. [[CrossRef](#)]
30. Weisz, E.; Huang, H.L.; Li, J.; Borbas, E.E.; Baggett, K.; Thapliyal, P.; Guan, L. International MODIS and AIRS Processing Package: AIRS Products And Applications. *J. Appl. Remote Sens.* **2007**, *1*. [[CrossRef](#)]
31. Weisz, E.; Smith, W.L.; Smith, N. Advances in Simultaneous Atmospheric Profile and Cloud Parameter Regression Based Retrieval from High-Spectral Resolution Radiance Measurements. *J. Geophys. Res. Atmos.* **2013**, *118*, 6433–6443. [[CrossRef](#)]
32. Milstein, A.B.; Blackwell, W.J. Neural Network Temperature and Moisture Retrieval Algorithm Validation for AIRS/AMSU and CrIS/ATMS: NEURAL NETWORK T AND Q VALIDATION. *J. Geophys. Res. Atmos.* **2016**, *121*, 1414–1430. [[CrossRef](#)]

33. Blackwell, W.J.; Milstein, A.B. A Neural Network Retrieval Technique for High-Resolution Profiling of Cloudy Atmospheres. *IEEE J. Sel. Top. Appl. Earth Obs. Remote Sens.* **2014**, *7*, 1260–1270. [[CrossRef](#)]
34. Chahine, M.T. Remote Sensing of Cloud Parameters. *J. Atmos. Sci.* **1982**, *39*, 159–170. [[CrossRef](#)]
35. Rosenkranz, P.W.; Barnet, C.D. Microwave Radiative Transfer Model Validation. *J. Geophys. Res.* **2006**, *111*. [[CrossRef](#)]
36. Rosenkranz, P.W. Rapid Radiative Transfer Model for AMSU/HSB Channels. *IEEE Trans. Geosci. Remote Sens.* **2003**, *41*, 362–368. [[CrossRef](#)]
37. Haines, D.A. A Lower Atmospheric Severity Index for Wildland Fire. *Natl. Weather Dig.* **1988**, *13*, 23–27.
38. Werth, P.; Ochoa, R. The Evaluation of Idaho Wildfire Growth Using the Haines Index. *Wea. Forecast.* **1993**, *8*, 223–234. [[CrossRef](#)]
39. Ziemke, J.R.; Chandra, S.; Labow, G.J.; Bhartia, P.K.; Froidevaux, L.; Witte, J.C. A Global Climatology of Tropospheric and Stratospheric Ozone Derived from Aura OMI and MLS Measurements. *Atmos. Chem. Phys.* **2011**, *11*, 9237–9251. [[CrossRef](#)]
40. Van Haver, P.; De Muer, D.; Beekmann, M.; Mancier, C. Climatology of Tropopause Folds At Midlatitudes. *Geophys. Res. Lett.* **1996**, *23*, 1033–1036. [[CrossRef](#)]
41. Thouret, V.; Cammas, J.-P.; Sauvage, B.; Athier, G.; Zbinden, R.; Nédélec, P.; Simon, P.; Karcher, F. Tropopause Referenced Ozone Climatology and Inter-Annual Variability (1994–2003) from the MOZAIC programme. *Atmos. Chem. Phys.* **2006**, *6*, 1033–1051. [[CrossRef](#)]
42. HWT Blog. ILX Upper-Air Sounding Comparison to NUCAPS and Modified NUCAPS. The Satellite Proving Ground at the Hazardous Weather Testbed 2019. Available online: <http://goesrhwt.blogspot.com/2019/06/ilx-upper-air-sounding-comparison-to.html> (accessed on 19 July 2020).
43. HWT Blog. Springfield Illinois Storms. Spring Experiments and Beyond 2019. Available online: <https://inside.nssl.noaa.gov/ewp/2019/06/05/springfield-illinois-storms/> (accessed on 17 July 2020).
44. Storm Prediction Center Storm Prediction Center Storm Reports. Available online: https://www.spc.noaa.gov/climo/reports/190605_rpts.html (accessed on 19 July 2020).
45. Dostalek, J.F.; Haynes, J.; Lindsey, D. NUCAPS Boundary Layer Modifications in Pre-convective Environments: Development of a Timely and More Accurate Product to Assist Forecasters in Making Severe Weather Forecasts. In *2019 JPSS Science Digest*; NOAA NASA Joint Polar Satellite System Program: Greenbelt, MD, USA, 2019.
46. Smith, N.; Esmaili, R.B.; Barnet, C.D.; Frost, G.J.; McKeen, S.A.; Trainer, M.K.; Francoeur, C. Monitoring atmospheric composition and long-range smoke transport with NUCAPS Satellite Soundings in Field Campaigns and Operations. In *Proceedings of the 100th American Meteorological Society Annual Meeting*, Boston, MA, USA, 12–16 January 2020.
47. Fuell, K. Introduction to NUCAPS Products for Fire Weather Potential. Available online: <https://nasasporttraining.wordpress.com/2020/03/10/introduction-to-nucaps-products-for-fire-weather-potential/> (accessed on 27 July 2020).
48. Lindley, T.T.; Bowers, B.R.; Murdoch, G.P.; Smith, B.R.; Gitro, C.M. Fire-effective Low-level Thermal Ridges on the Southern Great Plains. *J. Oper. Meteorol.* **2017**, *5*, 146–160. [[CrossRef](#)]
49. National Interagency Coordination Center Wildland Fire Summary and Statistics Annual Report 2018. Available online: https://www.predictiveservices.nifc.gov/intelligence/2018_statsumm/intro_summary18.pdf (accessed on 1 October 2020).
50. Prospero, J.M.; Carlson, T.N. Vertical and Areal Distribution of Saharan dust Over the Western Equatorial North Atlantic Ocean. *J. Geophys. Res.* **1972**, *77*, 5255–5265. [[CrossRef](#)]
51. Kuciauskas, A.P.; Xian, P.; Hyer, E.J.; Oyola, M.I.; Campbell, J.R. Supporting Weather Forecasters in Predicting and Monitoring Saharan Air Layer Dust Events as They Impact the Greater Caribbean. *Bull. Am. Meteorol. Soc.* **2018**, *99*, 259–268. [[CrossRef](#)]
52. Carlson, T.N. The Saharan Elevated Mixed Layer and its Aerosol Optical Depth. *TOASCJ* **2016**, *10*, 26–38. [[CrossRef](#)]
53. Dunion, J.P.; Marron, C.S. A Reexamination of the Jordan Mean Tropical Sounding Based on Awareness of the Saharan Air Layer: Results from 2002. *J. Clim.* **2008**, *21*, 5242–5253. [[CrossRef](#)]

54. Kuciauskas, A.; Esmaili, R.B.; Reale, T.; Nalli, N.R. Using NUCAPS to Observe the Thermodynamic Structure of Strong Saharan Air Layer Outbreaks about its Source within the Deserts of Northeast Africa. In Proceedings of the 16th Annual Symposium on New Generation Operational Environmental Satellite Systems Session 11A How JPSS and GOES-R Coupled Resources Improve Forecasting, Boston, MA, USA, 12–16 January 2020; p. 4.
55. Dunion, J.P.; Velden, C.S. The Impact of the Saharan Air Layer on Atlantic Tropical Cyclone Activity. *Bull. Am. Meteorol. Soc.* **2004**, *85*, 353–366. [[CrossRef](#)]
56. Lara, M. Heterogeneity of Childhood Asthma Among Hispanic Children: Puerto Rican Children Bear a Disproportionate Burden. *Pediatrics* **2006**, *117*, 43–53. [[CrossRef](#)]
57. Jenkins, G.S.; Robjhon, M.L.; Smith, J.W.; Clark, J.; Mendes, L. The influence of the SAL and Lightning on Tropospheric Ozone Variability Over the Northern Tropical Atlantic: Results from Cape Verde during 2010. *Geophys. Res. Lett.* **2012**, *39*, 2012GL053532. [[CrossRef](#)]
58. Jenkins, G.S.; Robjhon, M.L.; Demoz, B.; Stockwell, W.R.; Ndiaye, S.A.; Drame, M.S.; Gueye, M.; Smith, J.W.; Luna-Cruz, Y.; Clark, J.; et al. Multi-Site Tropospheric Ozone Measurements Across the North Tropical Atlantic during the summer of 2010. *Atmos. Environ.* **2013**, *70*, 131–148. [[CrossRef](#)]
59. Grasso, L.; Bikos, D.; Torres, J.; Dostalek, J.F.; Wu, T.-C.; Forsythe, J.; Cronk, H.; Seaman, C.; Miller, S.; Berndt, E.B.; et al. Satellite Imagery and Products of the 16–17 February 2020 Saharan Air Layer Dust Event over the Eastern Atlantic: Impacts of Water Vapor on Dust Detection and Morphology. *Atmos. Meas. Tech.* **2020**, 1–33, in review. [[CrossRef](#)]
60. Reiter, E.R.; Nania, A. Jet-Stream Structure and Clear-Air Turbulence (CAT). *J. Appl. Meteorol.* **1964**, *3*, 247–260. [[CrossRef](#)]
61. Shapiro, M.A. Turbulent Mixing within Tropopause Folds as a Mechanism for the Exchange of Chemical Constituents between the Stratosphere and Troposphere. *J. Atmos. Sci.* **1980**, *37*, 994–1004. [[CrossRef](#)]
62. Danielsen, E.F. Stratospheric-Tropospheric Exchange Based on Radioactivity, Ozone and Potential Vorticity. *J. Atmos. Sci.* **1968**, *25*, 502–518. [[CrossRef](#)]
63. Fuell, K.; LeRoy, A. Gridded NUCAPS Daily Applications of Satellite Soundings. Available online: <https://nasasporttraining.wordpress.com/2020/08/25/gridded-nucaps-daily-applications-of-satellite-soundings/> (accessed on 27 August 2020).
64. University of Wyoming College of Engineering Department of Atmospheric Science Upper Air Sounding Archive. Available online: <http://weather.uwyo.edu/upperair/sounding.html> (accessed on 19 July 2020).
65. EUMETSAT. User Services Division. Best-Practices for RGB Compositing Multi-Spectral Imagery. Available online: http://oiswww.eumetsat.int/~jids/html/doc/best_practices.pdf (accessed on 19 July 2020).
66. EUMETSAT. Airmass RGB. Available online: http://oiswww.eumetsat.int/~jids/html/doc/airmass_interpretation.pdf (accessed on 19 July 2020).
67. Lensky, I.M.; Rosenfeld, D. Clouds-Aerosols-Precipitation Satellite Analysis Tool (CAPSAT). *Atmos. Chem. Phys.* **2008**, *8*, 6739–6753. [[CrossRef](#)]
68. Berg, R. National Hurricane Center Tropical Cyclone Report Hurricane Arthur (AL012014). Available online: https://www.nhc.noaa.gov/data/tcr/AL012014_Arthur.pdf (accessed on 19 July 2020).
69. Berndt, E.B. JPSS Satellite Products for Extratropical Transition. Available online: <https://nasasporttraining.wordpress.com/2016/07/21/jpss-satellite-products-for-extratropical-transition/> (accessed on 20 August 2020).
70. Lindstrom, S. CIMSS Satellite Blog. Can You Use NUCAPS Soundings to Determine the Rain/Snow Line? Available online: <https://cimss.ssec.wisc.edu/satellite-blog/archives/35383> (accessed on 15 June 2020).
71. Duran, P.; Duran, E. The Wide World of SPoRT. SPoRT Provides Forecasts of Hurricane Isaias' Landfall to NOAA's Hurricane Research Division. Available online: <https://nasasport.wordpress.com/2020/08/13/sport-provides-forecasts-of-hurricane-isaias-landfall-to-noaas-hurricane-research-division/> (accessed on 14 August 2020).
72. Lindstrom, S. CIMSS Satellite Blog. Dry Air in the southwest Atlantic. Available online: <https://cimss.ssec.wisc.edu/satellite-blog/archives/37767> (accessed on 30 July 2020).
73. Duran, E. The Wide World of SPoRT. Exploring Daily Changes in Tropical Cyclone Temperature and Moisture using NUCAPS Satellite Soundings. Available online: <https://nasasport.wordpress.com/2020/08/20/exploring-daily-changes-in-tropical-cyclone-temperature-and-moisture-using-nucaps-satellite-soundings/> (accessed on 21 August 2020).

74. Blackwell, W.J.; Braun, S.; Bennartz, R.; Velden, C.; DeMaria, M.; Atlas, R.; Dunion, J.; Marks, F.; Rogers, R.; Annane, B.; et al. An overview of the TROPICS NASA Earth Venture Mission. *Q. J. R. Meteorol. Soc.* **2018**, *144*, 16–26. [[CrossRef](#)]
75. Kalmus, P.; Kahn, B.H.; Freeman, S.W.; van den Heever, S.C. Trajectory-Enhanced AIRS Observations of Environmental Factors Driving Severe Convective Storms. *Mon. Wea. Rev.* **2019**, *147*, 1633–1653. [[CrossRef](#)]



© 2020 by the authors. Licensee MDPI, Basel, Switzerland. This article is an open access article distributed under the terms and conditions of the Creative Commons Attribution (CC BY) license (<http://creativecommons.org/licenses/by/4.0/>).